

# Control on stratospheric temperature in IFS: resolution and vertical advection

I. Polichtchouk, Tim Stockdale, Peter  
Bechtold, Michail Diamantakis, Sylvie  
Malardel, Irina Sandu, Filip Vana, Nils  
Wedi

Research Department

June 10, 2019

*This paper has not been published and should be regarded as an Internal Report from ECMWF.  
Permission to quote from it should be obtained from the ECMWF.*



European Centre for Medium-Range Weather Forecasts  
Europäisches Zentrum für mittelfristige Wettervorhersage  
Centre européen pour les prévisions météorologiques à moyen terme

Series: ECMWF Technical Memoranda

A full list of ECMWF Publications can be found on our web site under:

<http://www.ecmwf.int/en/research/publications>

Contact: [library@ecmwf.int](mailto:library@ecmwf.int)

©Copyright 2019

European Centre for Medium-Range Weather Forecasts  
Shinfield Park, Reading, RG2 9AX, England

Literary and scientific copyrights belong to ECMWF and are reserved in all countries. This publication is not to be reprinted or translated in whole or in part without the written permission of the Director-General. Appropriate non-commercial use will normally be granted under the condition that reference is made to ECMWF.

The information within this publication is given in good faith and considered to be true, but ECMWF accepts no liability for error, omission and for loss or damage arising from its use.

## Abstract

All operational forecast systems at ECMWF suffer from lower tropical stratosphere cold bias, which has a distinctive resolution dependency. At typical vertical resolutions of the ECMWF Integrated Forecasting System ( $\sim 450\text{m}$  or  $\sim 350\text{m}$  in the lower stratosphere), the lower stratospheric cold bias is increased when the horizontal resolution is increased, while the upper stratospheric warm bias is concomitantly reduced. This is because the stratosphere cools in the global-mean when horizontal resolution is increased. The cooling is due to discretization errors in the vertical advection, associated with inadequate representation of resolved gravity waves in the vertical direction. Although for typical climate model resolutions this problem is negligible, for high resolution numerical weather prediction systems this is a serious problem. It is shown that an increase in i) the vertical resolution and/or 2) the order of semi-Lagrangian vertical interpolation reduce the temperature sensitivity to horizontal resolution via better representation of gravity waves in the vertical direction. It is alternatively shown that filtering grid-point temperature oscillations in the vertical direction alleviates the global-mean cooling of the stratosphere at high horizontal resolutions.

## 1 Introduction to the problem

Forecast skill scores are expected to improve as the resolution of a numerical weather prediction (NWP) model increases. However, in the ECMWF Integrated Forecast System (IFS) forecast skill scores degrade in the 100 to 50 hPa region at higher horizontal resolution. This is because IFS experiences a reduction in global-mean temperature in the stratosphere (Shepherd et al. 2018). As the upper stratosphere in IFS is biased warm and the lower stratosphere is biased cold (see Fig. 9 in Shepherd et al. (2018); also see Fig. 4 ahead), the lower-to mid-stratospheric cold bias is exacerbated, whilst the upper stratospheric warm bias is alleviated to some extent, as a result of an increase in horizontal resolution. The focus of this report is to elucidate this resolution sensitivity, and if possible, eliminate it. Such a behaviour is undesirable for model development and tuning <sup>1</sup>.

The cooling in the lower stratosphere with horizontal resolution increase can be seen in Fig. 1, which shows the drift in zonal-mean temperature (with respect to high resolution operational analysis) for medium-range forecasts started on each day at 00UTC in December (top) and July (bottom) in CY43R3<sup>2</sup>. The cooling at 50 hPa occurs at all latitudes — i.e., there is a global-mean cooling — and is larger for high horizontal resolutions. For example, compare the drift in the TCo1279 horizontal resolution ( $\sim 9$  km grid spacing) forecasts (black line) to TCo399 horizontal resolution ( $\sim 30$  km grid spacing) forecasts (pink line in the top panel, and brown line in the bottom panel) at L137 vertical resolution. The seasonal ensemble prediction system (henceforth SEAS5) shows the same behaviour for the global-mean temperature at 70 hPa in Fig. 2. This figure further shows that the cooling saturates on a time scale of few months, which is the radiative timescale in the lower stratosphere. Both figures also reveal that lower vertical resolution forecasts suffer from larger decrease in global-mean temperature for a given horizontal resolution (e.g., compare red line to green line in the top panel of Fig. 1, and, red line to dark blue line in Fig. 2).

A latitude-pressure cross section of the stratospheric temperature response to increase in horizontal resolution is shown in Fig. 3 for medium-range forecasts. The figure shows that the cooling with the increase in horizontal resolution is strongest in the tropics and in the summer hemisphere. Figure 4 shows the horizontal resolution sensitivity of temperature bias in JJA in SEAS5. Since the horizontal resolution

<sup>1</sup>For example, changes to the radiation scheme discussed in Hogan et al. (2017), which improve the upper stratospheric and mesospheric warm bias, slightly increase the lower- to mid- stratospheric cold bias. This degradation is larger at high horizontal resolution and therefore prevents the otherwise beneficial radiation changes from being implemented operationally in the IFS.

<sup>2</sup>This behaviour is not limited to CY43R3, and is present in later and earlier model cycles.

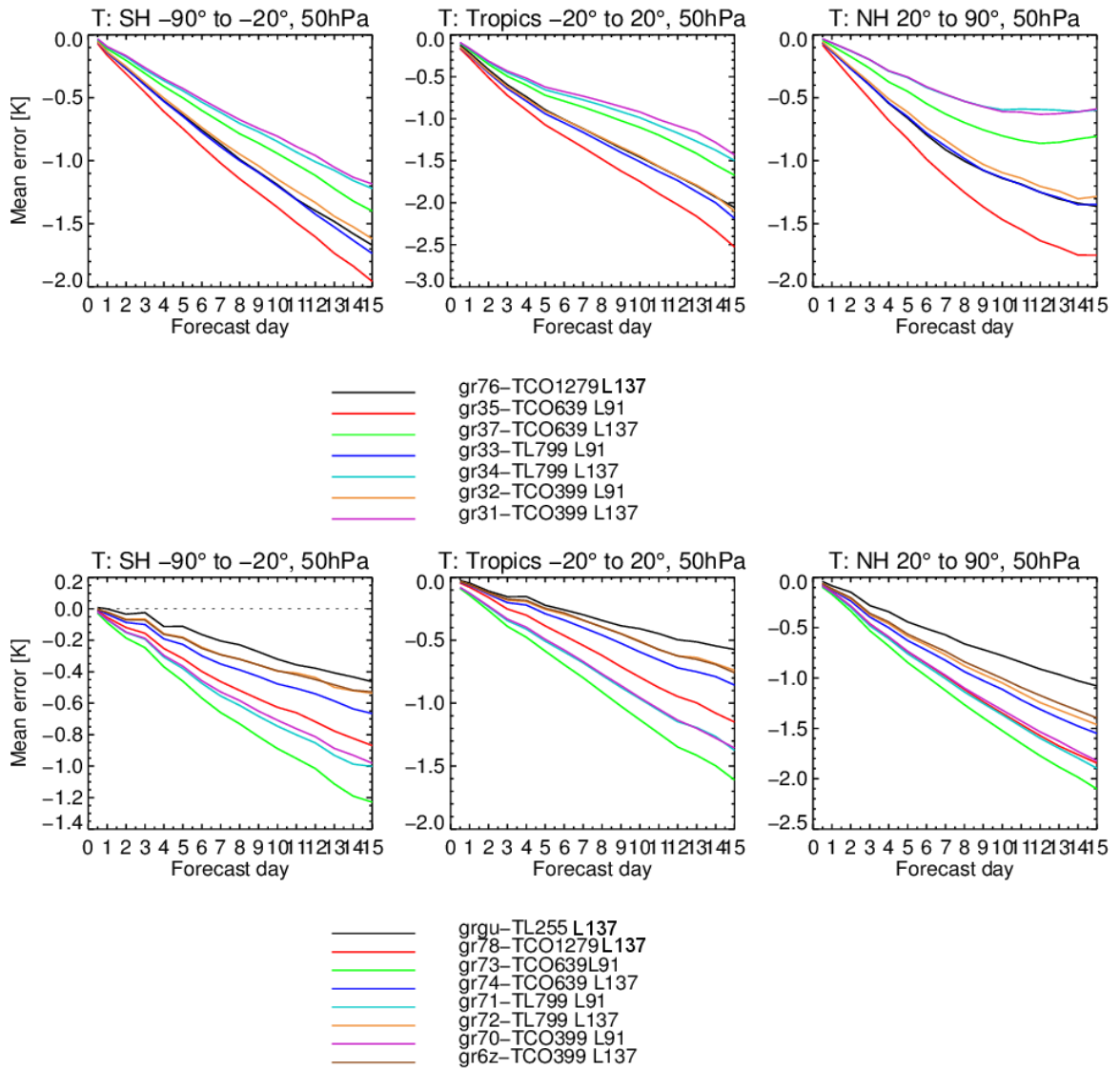


Figure 1: Regional temperature error verified against operational high resolution (HRES) analysis at 50 hPa for medium-range forecasts started each day at 00UTC in December (top) and July (bottom) 2016 in CY43R3. Different color lines show forecasts at different horizontal and vertical resolutions. “T” denotes horizontal resolution, and “L” vertical. For example, “TCO639L91” stands for cubic octahedral grid at 639 spectral truncation, with 91 vertical levels; “TL799L137” stands for Gaussian linear grid at 799 spectral truncation, with 137 vertical levels.

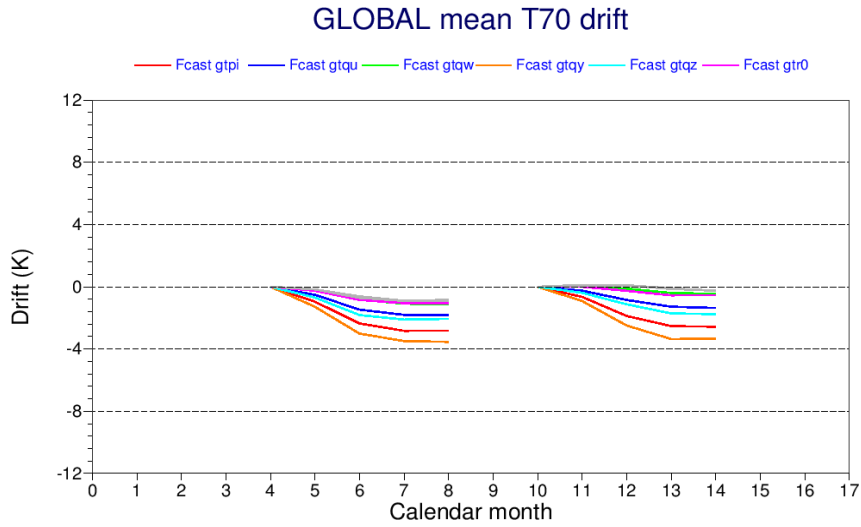


Figure 2: 70 hPa temperature error in SEAS5 as a function of resolution. Red and orange are TCo199L91 and TCo319L91; dark blue and light blue are TCo199L137 and TCo319L137; green and pink are TCo199L198 and TCo319L198; both grey lines are TCo199L320 and TCo319L320.

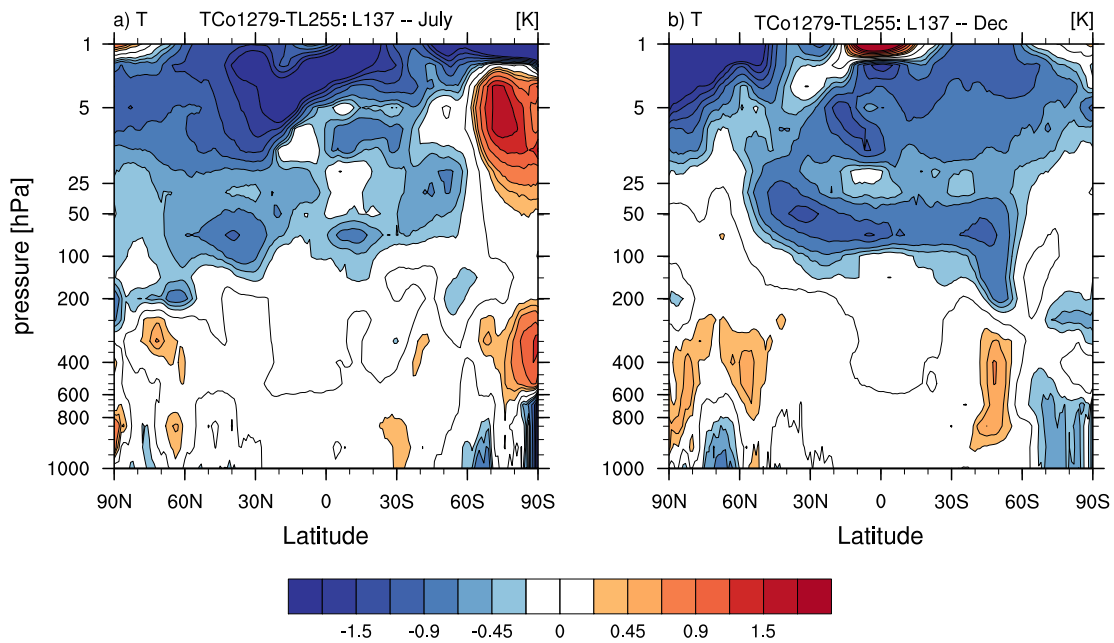


Figure 3: Latitude-pressure cross sections of zonal-mean temperature difference between TCo1279L137 and TL255L137 resolutions at a lead time of 10 days in (a) July and (b) December 2016. The mean over 31 forecasts is shown.

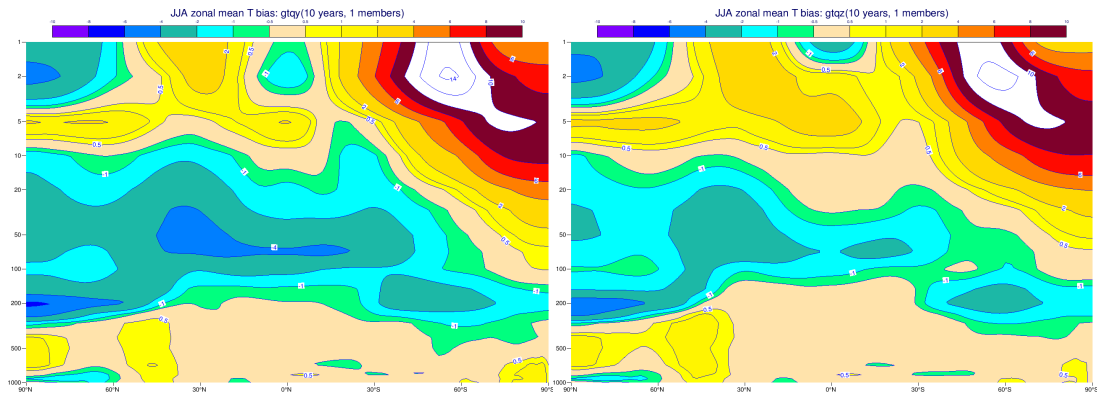


Figure 4: Latitude-pressure cross sections of JJA zonal-mean temperature bias against ERA-I (2001-2010, control member) for TCo319 (left) and TCo199 (right) seasonal experiments with 137 levels.

sensitivity is present for all forecast ranges and in all seasons, this report focuses on understanding the resolution sensitivity in medium-range forecasts in July.

This report is structured as follows. Section 2 shows that the cooling observed when the horizontal resolution is increased comes from the dynamical core, and in particular, from the discretization errors in vertical advection, brought about by inadequate representation of resolved gravity waves in the vertical direction. Section 3 presents solutions on how the horizontal resolution sensitivity of global-mean temperature can be reduced via 1) an increase in the vertical resolution; 2) an increase in the order of semi-Lagrangian vertical temperature interpolation; and 3) filtering grid scale waves in the vertical direction in the temperature field. This section also gives theoretical arguments for why an increase in horizontal resolution should be accompanied by an increase in vertical resolution (and/or more accurate treatment of the vertical advection). Section 4 shows the impact on forecast skill scores of the solutions proposed in section 3. Finally, summary, conclusions and recommendations are given in section 5.

## 2 Dynamical core

It is natural to ask whether the increase in the global-mean cooling observed at higher horizontal resolution is caused by the resolution sensitivity of the resolved or parametrized processes. To address this, 10-day forecasts for July are performed at TL255 and TCo1279 horizontal resolutions ( $\sim 80$  km and  $\sim 9$  km, respectively), where all physical parameterizations and the wave model are switched off. The latitude-pressure distribution of the temperature response to the increase in horizontal resolution is shown in Fig. 5a. By comparing this figure to Fig. 3, it is clear that the resolution sensitivity is present, and is larger, in the absence of physical parameterizations. This suggests that the cooling with horizontal resolution increase is due to the dynamical core.

That the cooling is coming from the dynamical core can be further verified by running the full forecasts (i.e., with all the parameterizations switched on) and examining the temperature tendencies from the parametrized processes and the dynamical core (before applying the semi-implicit correction, the hyperviscosity and the sponge). The parametrized processes affecting the temperature budget are radiation, clouds and convection, vertical diffusion, and, heating by dissipating gravity waves. The combined effect of these parametrized processes is called the ‘total physics’ temperature tendency. The response to the increase in horizontal resolution in the ‘dynamics’ and the total physics temperature tendencies is shown in Fig. 6, together with the temperature response for forecasts at lead time of 3 days. It is clear that

the difference in the dynamics tendencies can explain the total cooling observed when increasing the horizontal resolution. From this, two other conclusions can be drawn: 1) The lack of response in the radiation tendency (not shown) indicates that the cooling can not be attributed to an increase in water vapour transport into the stratosphere at higher horizontal resolution that would result in an increase in longwave cooling; and 2) dynamical core tendencies from semi-implicit correction, the hyper-viscosity and the sponge — which are not included in the dynamics tendency shown in Fig. 6a— are not the leading order terms behind the horizontal resolution sensitivity.

As the horizontal resolution is increased, a larger part of the gravity wave spectrum is resolved and more energy is present in the stratosphere in the divergent part of the kinetic energy spectrum. This is shown in Fig. 7. The transition to the divergence dominated regime occurs for total wavenumbers  $N$  greater than  $\sim 20$  (cf. thin lines to thick blue line in Fig. 7). However, the difference in the divergent kinetic energy spectrum between low (TL255) and high (TCo1279) horizontal resolutions can be seen for  $N > 40$ : There is considerable less energy in total wavenumbers  $40 < N < 255$  at low horizontal resolution (cf. thin black line to thin blue line in Fig. 7). More energy in the divergent part of the spectrum indicates more gravity wave activity.

To test if more gravity wave activity at higher horizontal resolution is the reason for the global-mean cooling, additional forecasts were performed at TCo1279 and TL255 horizontal resolutions, in which a strong damping on the divergence field was applied from 150 hPa upwards in order to eliminate resolved gravity waves in the stratosphere. Note that in the current operational IFS, a strong divergence damping (i.e., the “sponge”) is applied from at 1 hPa upwards to filter out gravity waves and prevent wave reflection from the upper boundary.

That filtering out gravity waves in the lower to mid stratosphere (i.e., applying the “deep sponge”), helps to alleviate the horizontal resolution temperature sensitivity can be seen by comparing Fig. 5b to Fig. 3a. Moreover, the filtering impacts higher horizontal resolution more than the lower horizontal resolution (Fig. 5c vs Fig. 5d). Further tests where the divergence damping was restricted to a specified total wavenumber range indicate that total wavenumbers  $40 < N < 300$  are responsible for this cooling (not shown). This indicates that the representation of resolved gravity waves with horizontal wavelengths of  $\mathcal{O}(50 - 500\text{km})$  is the reason for the global-mean cooling at high horizontal resolution with the current operational distribution of vertical levels. It should be emphasised that the total wavenumbers  $40 < N < 300$  are not close to the truncation scale of the TCo1279 resolution. Therefore, further tests at TCo1279 where the hyper-dissipation —designed to remove energy near the truncation scale—was increased to that of TL255 resolution, showed no sensitivity in the global-mean temperature.

Several mechanisms exist via which an increase in gravity wave activity at higher horizontal resolution in  $40 < N < 300$  could lead to temperature changes: 1) via an increase in gravity wave drag and a concomitant increase in adiabatic cooling via strengthened residual-mean meridional circulation; 2) via an increase in eddy forcing terms in the thermodynamic equation (see ahead to equation 1); and, 3) via discretization errors and non-conservation in the dynamical core.

From the spatial structure of the resolution dependence in Figs. 3 and 5a (i.e., with warming over the winter pole and cooling elsewhere), there is some evidence that 1) could be playing a role. However, we need a careful examination of the model output to establish if this, or the other two possibilities may be at play. To do this, let us examine the horizontal resolution sensitivity of terms in the transformed Eulerian-mean (TEM) thermodynamic equation in pressure  $p$ -coordinates (Andrews et al. 1987):

$$\bar{\theta}_t + a^{-1} \bar{v}^* \bar{\theta}_\phi + \bar{\omega}^* \bar{\theta}_p - \bar{Q} = -[\bar{v}' \theta' \bar{\theta}_\phi / a \bar{\theta}_p + \bar{\omega}' \theta']_p, \quad (1)$$

where  $\theta = T(p/p_0)^\kappa$  is the potential temperature, with  $\kappa = R/c_p$ ,  $R$  the gas constant, and,  $c_p$  the specific heat at constant pressure;  $a$  is the radius of the Earth;  $Q$  comprises of diabatic heating (i.e., the radiation)

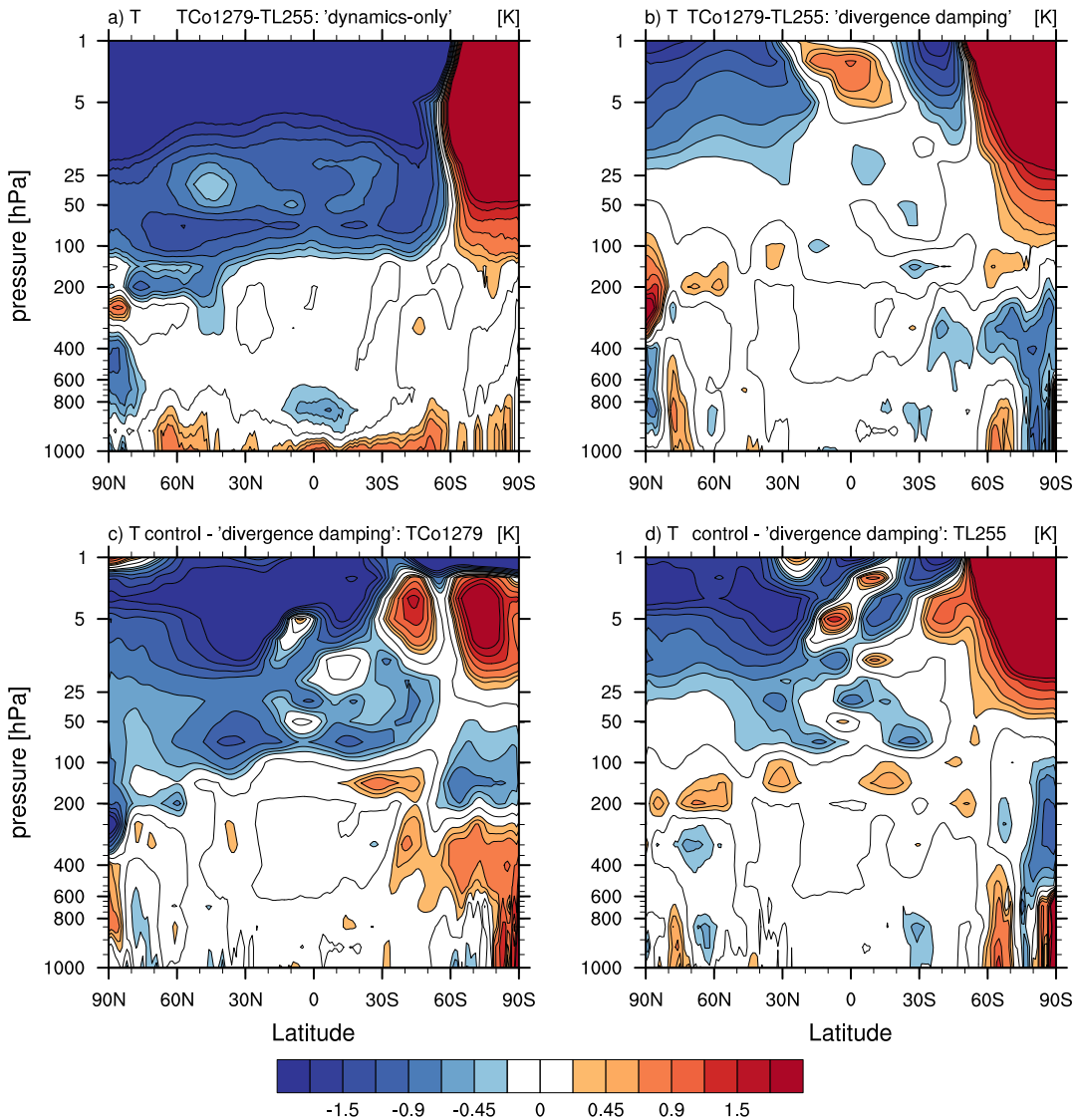


Figure 5: Latitude-pressure cross sections of zonal-mean temperature response to an increase in horizontal resolution from TL255 to TCo1279. (a) ‘Dynamics only’ forecasts, and, (b) ‘divergence damping in the stratosphere’ forecasts (see text) at lead time of 10 days in July. The mean over 31 start dates in July 2016 is shown. Difference between the control forecast and the divergence damping forecast at (c) TCo1279 and (d) TL255 horizontal resolutions. Notice the larger impact of divergence damping in the lower stratosphere at high horizontal resolution.

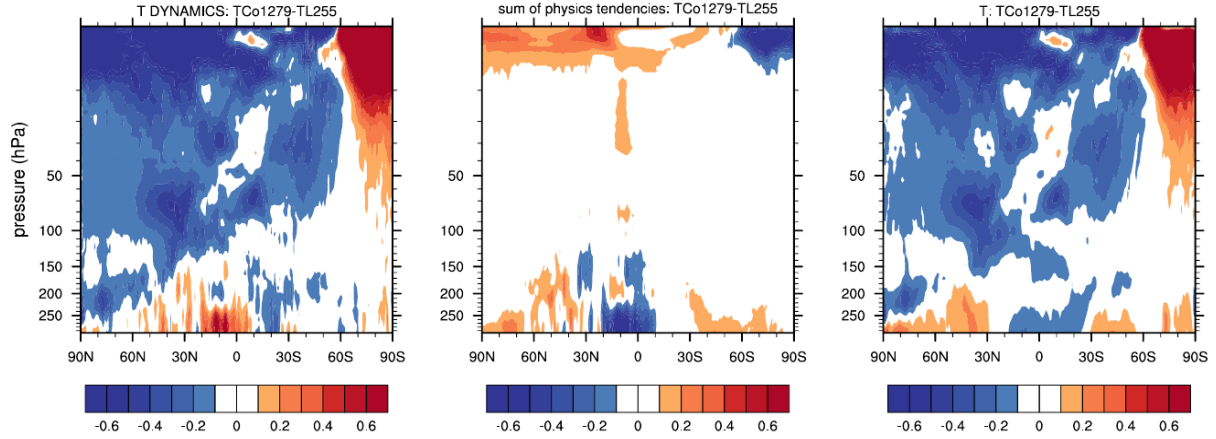


Figure 6: Latitude-pressure cross sections of response in the accumulated zonal-mean temperature tendency [in  $K/s \times 3$  days] to horizontal resolution increase (from TL255 to TCo1279) due to (a) dynamics and (b) total physics. (c) Temperature response [in K] to horizontal resolution increase (from TL255 to TCo1279). Mean over ‘full physics’ July forecasts at lead time of three days are shown.

and other parametrized processes; and  $\bar{v}^*$  and  $\bar{\omega}^*$  is the residual-mean meridional circulation:

$$\bar{v}^* \equiv \bar{v} - (\overline{v'\theta'}/\bar{\theta}_p)_p \quad (2)$$

$$\bar{\omega}^* \equiv \bar{\omega} + (a \cos \phi)^{-1} (\cos \phi \overline{v'\theta'}/\bar{\theta}_p)_\phi, \quad (3)$$

where  $v$  is meridional wind, and,  $\omega = Dp/Dt$  is the vertical pressure velocity. As  $Q$  (i.e. the ‘‘physics’’) was shown not to be important for the global-mean cooling at higher horizontal resolution (see Fig. 6), the only terms that can modify  $\theta$  are i) the residual mean meridional circulation  $a^{-1}\bar{v}^*\bar{\theta}_\phi + \bar{\omega}^*\bar{\theta}_p$  and ii) eddy forcing term  $[\overline{v'\theta'}/a\bar{\theta}_p + \overline{\omega'\theta'}]_p$ . It should be noted that the second term in the eddy forcing term is the convergence of gravity wave heat flux, which dominates in the stratosphere over the first term (not shown). The primes refer to eddies. Because we will be comparing terms i) and ii) between TCo1279 and TL255 horizontal resolutions, an eddy is chosen to mean a physical space representation of a variable with total wavenumbers  $40 < N < 255$ . In practice, the  $\bar{\omega}^*$  term dominates the residual mean meridional circulation. In the stratosphere, the residual circulation is predominantly upward in the tropics and downward over the winter pole. Upwelling is associated with adiabatic cooling and downwelling with adiabatic warming (see e.g., a schematic of the residual circulation in the middle atmosphere in Plumb (2002)).

Additionally, variation in static stability, which is proportional to  $\bar{\theta}_p$ , plays a role in the global-mean temperature budget (Fueglistaler et al. 2011). Therefore, it is also of interest to establish if  $\bar{\omega}^*\bar{\theta}_p$  changes when horizontal resolution increases.

By the downward control (Haynes et al. 1991),  $\bar{\omega}^*$  can also be computed as follows:

$$\bar{\omega}^* = \frac{H}{pa \cos \phi} \frac{\partial}{\partial \phi} \left\{ \cos \phi \int_p^0 \frac{D}{f - (a \cos \phi)^{-1} \partial(\bar{u} \cos \phi) / \partial \phi} \right\} dp', \quad (4)$$

where  $H$  is the scale height,  $f$  is the Coriolis parameter,  $\bar{u}$  is the mean zonal wind, and,  $D$  is the zonal-mean wave drag composed of the resolved and parametrized gravity wave drag. The contribution from the resolved gravity wave drag to  $D$  is

$$-\frac{\partial}{\partial p} \overline{\omega'u'}. \quad (5)$$

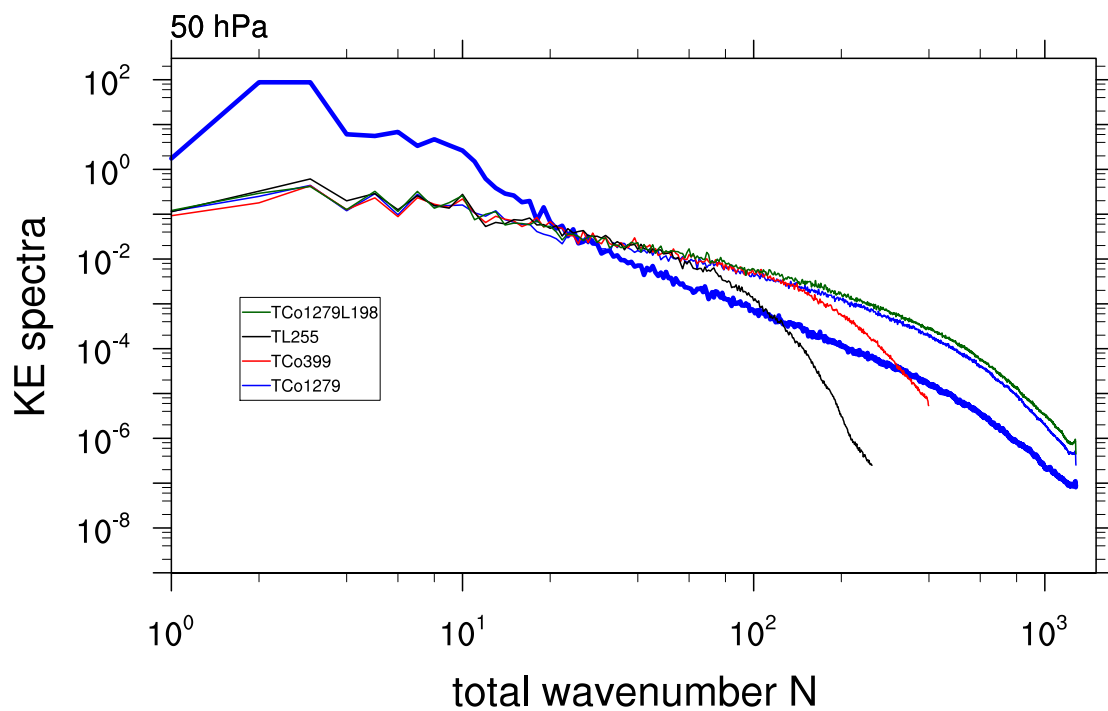


Figure 7: Kinetic energy spectrum at 50hPa. Thin lines show divergent kinetic energy spectrum at different resolutions: TL255L137 (black), TCo399L137 (red), TCo1279L137 (blue), and, TCo1279L198 (green). Thick blue line shows rotational kinetic energy spectrum at TCo1279L137 resolution. For total wavenumbers  $N > 20$ , divergent kinetic energy spectrum dominates in the stratosphere. Note the increase in wave energy with increase in vertical resolution (cf. green and blue thin lines).

It is conceivable that at high horizontal resolution, the resolved gravity wave drag from total wavenumbers  $40 < N < 300$  increases, leading to stronger  $\overline{\omega}^*$  and stronger adiabatic cooling in the tropics.

Let us now examine the change in the residual mean meridional circulation, the eddy forcing term in the thermodynamic equation, and, the resolved gravity wave drag, with an increase in horizontal resolution. This is shown in Fig. 8 (panels a-c). It is clear that the change in residual mean meridional circulation, or, the eddy forcing term can not explain the observed cooling when horizontal resolution is increased (cf. Fig. 8a-b to Fig. 3a). There is some indication of increased gravity wave drag at TCo1279. However, any increase in resolved drag appears to be completely compensated by the decrease in parametrized gravity wave drag (cf. Fig. 8c with Fig. 8d). Therefore, it is unlikely that mechanisms 1) or 2) proposed above, are responsible for the cooling observed when increasing the horizontal resolution. The change in  $\overline{\omega}^* \overline{\theta}_p$  is nearly-identical to Fig. 8a (not shown). Therefore change in static stability (proportional to  $\overline{\theta}_p$ ) can not be responsible for the global-mean cooling.

It should be further noted that an increase in residual circulation would lead to a concomitant warming over the winter pole, and, could not alone explain the global-mean cooling of the stratosphere at higher horizontal resolution. This leads us to conclude that the discretization errors in the dynamical core are the reason for this unphysical behaviour. Further evidence for this is provided in the Appendix, where results from adiabatic dry, idealized gravity wave propagation experiments also show a global-mean cooling with an increase in horizontal resolution. This is so even in the absence of critical and/or shear layers and with no explicitly applied numerical damping. Moreover, the cooling with an increase in horizontal resolution can also be observed in both the semi-Lagrangian and less diffusive Eulerian dynamical cores of the IFS (not shown). Therefore, not accounting for frictional heating due to removal of kinetic energy by diffusion (both explicit and implicit) in the dynamical core (Becker 2003), is an unlikely reason.

As the horizontal wavenumbers  $40 < N < 300$  driving the stratospheric cooling are well resolved in the horizontal direction at TCo1279 resolution, the likely culprit behind the cooling is the vertical advection. Indeed, Fig.2 already shows that an increase in the vertical resolution alleviates global-mean temperature sensitivity to horizontal resolution: This can be seen by e.g., comparing temperature drift for TCo199L91 (red line) and TCo319L91 (orange line) to temperature drift for TCo199L198 (green line) and TCo319L198 (pink line). In what follows theoretical reasons for why higher vertical resolution is needed when increasing the horizontal resolution are reviewed and the results from forecasts with higher vertical resolution presented.

### 3 Towards more accurate vertical advection

#### 3.1 Theoretical considerations

The appropriate vertical to horizontal resolution aspect ratio for atmospheric models has been discussed in many previous studies and recently reviewed in Waite (2016). It is reviewed here for completeness.

To resolve horizontal grid-scale quasi-geostrophic (QG) vortices, the aspect ratio should be consistent with (Lindzen & Fox-Rabinovitz 1989):

$$\frac{\Delta z}{\Delta x} \sim \frac{f}{\mathcal{N}}, \quad (6)$$

where  $\Delta z$  is the vertical grid spacing,  $\Delta x$  is the horizontal grid spacing,  $f$  is the Coriolis parameter, and  $\mathcal{N}$  is the Brunt-Väisälä buoyancy frequency. As the total wavenumbers  $40 < N < 300$ , responsible for the horizontal resolution sensitivity, fall partially into the synoptic scales characterized by balanced dynamics, this ratio might be relevant outside the tropics. If  $\Delta x$  is taken to represent horizontal grid

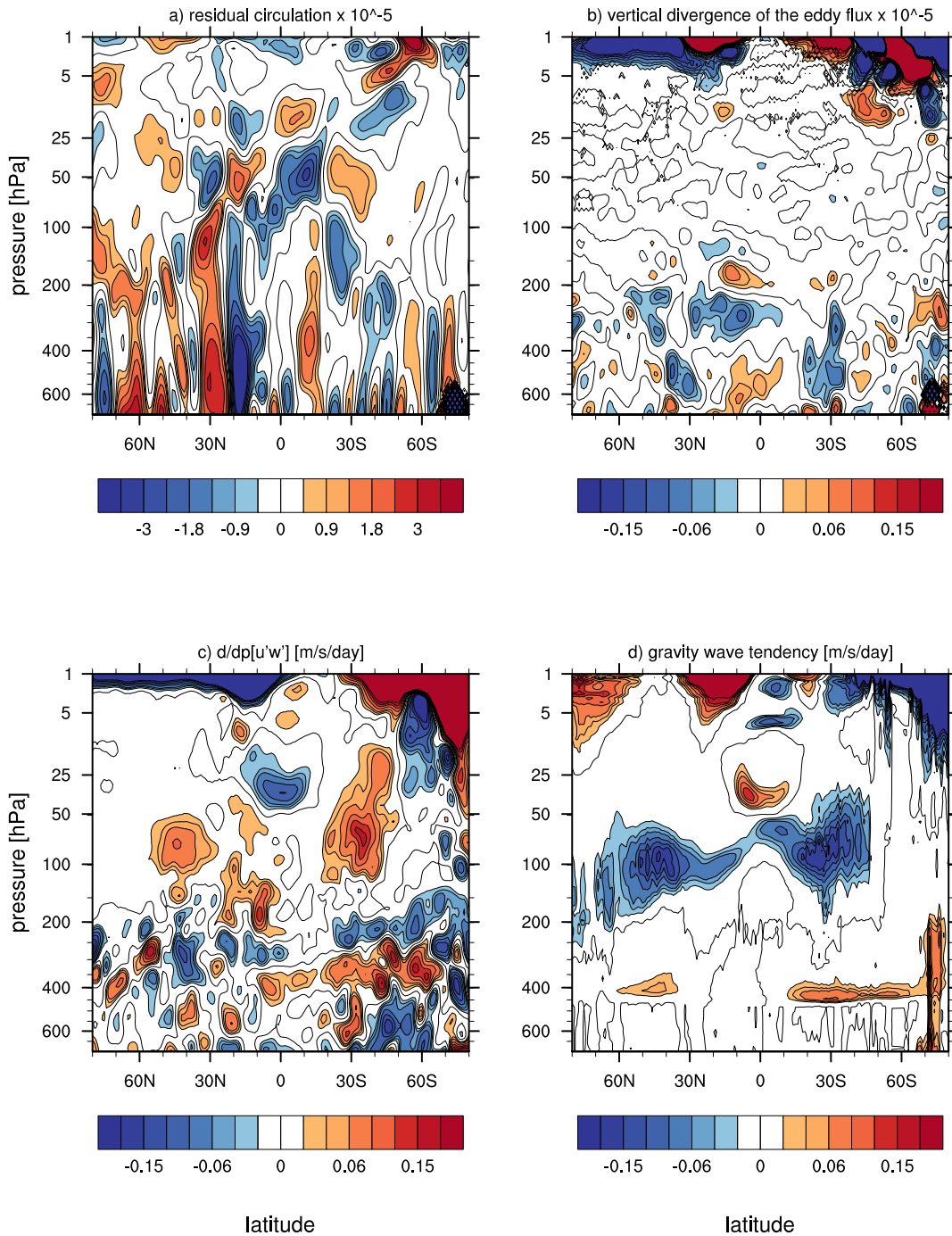


Figure 8: Latitude-pressure cross sections of zonal-mean potential temperature tendency [in K/s] difference (TCo1279-TL255) due to (a) residual mean-meridional circulation, and, (b) eddy forcing term in the thermodynamic equation (including the gravity wave heat flux convergence). Change in (c) resolved gravity wave drag [in m/s/day], and, (d) parametrized gravity wave drag [in m/s/day]. Time mean over 'full physics' forecasts valid at day three in July are shown. All the quantities have been computed on model levels.

spacing applicable to  $40 < N < 300$  (i.e.,  $\Delta x \sim 50\text{-}500\text{km}$ ), at mid-latitude this results in vertical resolution requirement of  $\Delta z \sim 100\text{-}1000\text{m}$ . For  $N = 1279$  (i.e.,  $\Delta x \sim 10\text{km}$ ), however, the vertical resolution requirement is  $\Delta z \sim 200\text{ m}$ .

Total wavenumbers  $40 < N < 300$  also fall within the mesoscale, characterized by stratified turbulence and gravity waves, both of which have different requirements for vertical resolution. For example, stratified turbulence has a  $-5/3$  energy spectrum like that observed in the lower stratosphere (e.g. [Nastrom & Gage 1985](#), [Bacmeister et al. 1996](#), [Burgess et al. 2013](#)). Stratified turbulence develops shear layers with thickness around the buoyancy scale  $L_b \equiv 2\pi U / \mathcal{N}$  ([Billant & Chomaz 2001](#), [Waite & Bartello 2004](#)), where  $U$  is a typical horizontal velocity scale. In the tropical lower stratosphere<sup>3</sup>,  $U \sim 5\text{ m s}^{-1}$  and  $\mathcal{N} > \epsilon \times \infty r^{-\epsilon}$  giving  $L_b \sim 1\text{km}$ . Therefore, to resolve such shear layers a vertical resolution of  $\sim 200\text{m}$  would be required (given that at least four grid points are needed to represent a wave).

In the lower- to mid- stratosphere, the unbalanced dynamics consists mainly of upward-propagating gravity waves ([Shepherd et al. 2018](#)). The gravity wave dispersion relation for hydrostatic medium frequency waves is (e.g., [Fritts & Alexander 2003](#))

$$\hat{\omega} = \mathcal{N} \left| \frac{\sqrt{k^2 + l^2}}{m} \right|, \quad (7)$$

where  $(k, l, m)$  are the zonal, meridional and vertical wavenumber components, and,  $\hat{\omega} \equiv \omega - k\bar{u} - l\bar{v}$  is the frequency that would be observed in a frame of reference moving with the background horizontal wind  $\bar{u}$  and  $\bar{v}$ . Or equivalently, (7) can be rewritten for vertical wavenumber  $m$

$$|m| = \frac{\mathcal{N}}{|\hat{c}_h|}, \quad (8)$$

where  $\hat{c}_h \equiv \hat{\omega}/k_h = (c_h - \bar{u}_h)$ , with  $k_h = \sqrt{k^2 + l^2}$ . Note that  $k_h > 0$  for  $\hat{c}_h > 0$ , and,  $k_h < 0$  for  $\hat{c}_h < 0$ . Thus the vertical wavenumber can be related to static stability and background winds. Moreover, for a given frequency and stratification, equation (7) implies that a decrease in the horizontal wavelength should be accompanied by a decrease in the vertical wavelength. This further emphasizes the need to increase vertical resolution with an increase in the horizontal resolution.

At the tropopause, a sharp transition between less stable tropospheric air and more stable stratospheric air occurs. The increase in  $\mathcal{N}$  is particularly pronounced in the tropics (see e.g., Figure 2 in [Birner et al. 2006](#)), where  $\mathcal{N}$  increases by more than a factor of two. Moreover, the climatological tropical horizontal winds change little at the tropopause. Therefore, from (8) the vertical wavelength of a gravity wave should shrink by a factor of two as the wave propagates from the troposphere into the stratosphere. As a result, a better vertical resolution would be needed in the stratosphere to model gravity wave propagation accurately. Estimates of vertical wavelength from MU Radar measurements in Japan indicate that the dominant vertical wavelengths in the lower stratosphere are 1-3 km ([Sato 1994](#)).

[Lindzen & Fox-Rabinovitz \(1989\)](#) state that inadequate vertical to horizontal resolution aspect ratio in models can lead to many undesired artefacts, such as ‘‘spatial instability’’, ‘‘incorrect solutions’’, and ‘‘other more complicated manifestations’’. Moreover,  $2\Delta z$  waves can be spuriously generated as a short vertical wavelength gravity wave can no longer be resolved by the vertical grid as it propagates into the stratosphere. [Untch & Hortal \(2004\)](#) showed that a vertical finite element scheme currently operational in IFS, suffers less from the presence of  $2\Delta z$  spurious waves in the stratosphere than the previously used finite difference formulation on the Lorenz grid. [Untch & Hortal \(2004\)](#) also showed that the cold bias

<sup>3</sup>For zonal wind climatology please see ERA-40 Atlas [https://software.ecmwf.int/static/ERA-40\\_Atlas/docs/section\\_D25/parameter\\_zmzwsp.html](https://software.ecmwf.int/static/ERA-40_Atlas/docs/section_D25/parameter_zmzwsp.html)

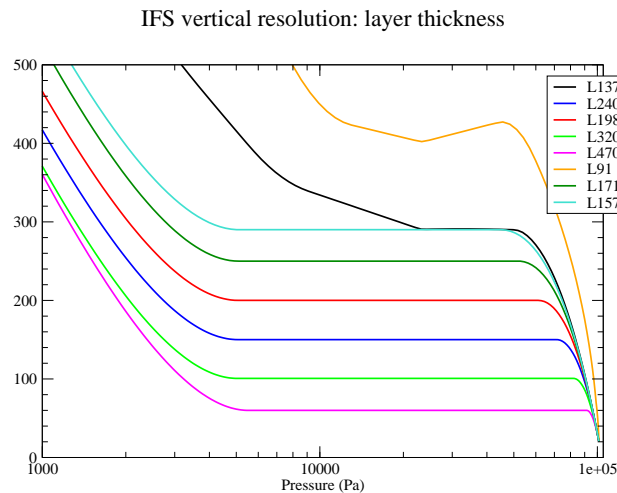


Figure 9: Approximate IFS vertical resolution [m] as a function of pressure [Pa]. The black line shows 137 level vertical resolution, which is used for the operational HRES. The orange line shows 91 level vertical resolution, which is operational in ENS and in SEAS5. Other curves show different vertical level configurations tested in this study.

in the lower stratosphere in IFS was markedly improved as a result of the move to the vertical finite elements. Indeed, it is found here that the use of the vertical finite elements markedly reduces horizontal resolution sensitivity of temperature in comparison to the finite difference scheme on the Lorenz grid (compare Fig. 25a to Fig. 25d in the Appendix). It is possible that an increase in vertical resolution further eradicates the spurious  $2\Delta z$  waves and therefore an investigation into the vertical resolution sensitivity of the global-mean temperature is warranted.

Let us now examine the vertical resolution in the IFS. Figure 9 shows approximate vertical resolutions (based on the standard atmosphere approximation) for the operational high resolution (HRES) 137 level configuration (in black), and operational medium-range ensemble prediction system (ENS) and SEAS5 91 level configuration (in orange). The vertical resolution reduces in the upper troposphere/lower stratosphere (UTLS) in both configurations, where the vertical coordinate is stretched at  $\sim 250$ hPa. In the 137-level (91-level) configuration, the vertical resolution degrades from 300m (400m) in the free troposphere to 400-500m (500-600m) in the lower- to mid-stratosphere. If at least four to six grid points are needed to represent a wave, the effective vertical resolution in the UTLS is  $>2$ km for the 137-level configuration and  $>3$ km for the 91-level configuration. From equation (8) and the discussion above, such stretching is undesirable for gravity wave propagation into the stratosphere. It should be noted that Wedi & Smolarkiewicz (2006) found that a quasi-biennial oscillation in the stratosphere was not produced with less than five grid points per vertical wavelength. Instead 10-15 grid points per vertical wavelength were needed to achieve convergence. Therefore, the four to six grid points quoted above is an optimistic estimate.

Given the above theoretical considerations, it is possible that the current vertical resolution in the stratosphere is too coarse for the higher TCo1279 horizontal resolution. To test what impact increasing vertical resolution has on the “cooling with horizontal resolution” problem, forecasts with increased vertical resolution in the lower- to mid- stratosphere were performed (see other curves in Fig. 9 for the vertical resolutions tested). The results are discussed in the following section.

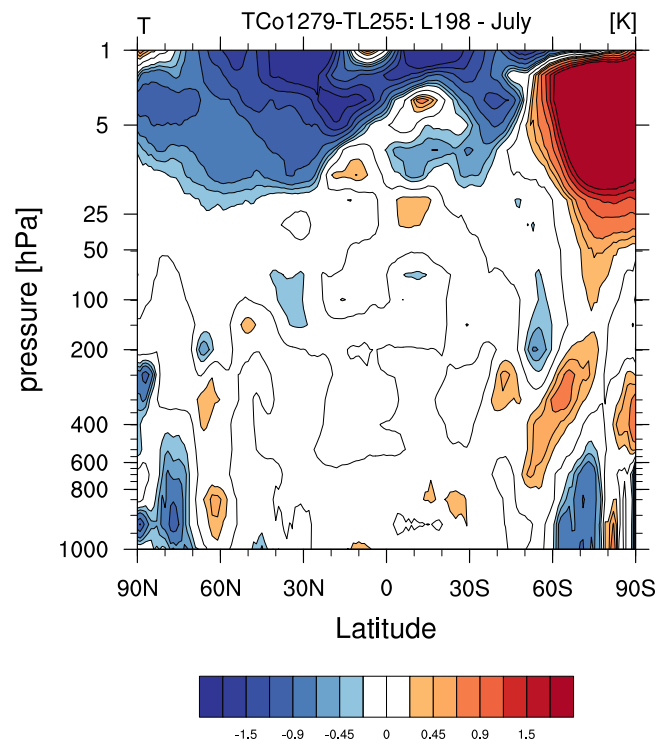


Figure 10: Same as Fig 3a, but at L198 vertical resolution.

### 3.2 Vertical resolution sensitivity experiments

Figure 10 shows the impact of increased vertical resolution (to 198 levels) on the horizontal resolution sensitivity of temperature. As can be seen from the figure, L198 vertical resolution — which implies 200m vertical grid spacing in the mid- to lower stratosphere — is enough to eliminate the horizontal resolution sensitivity, at least in forecasts at a lead time of 10 days (cf. Fig. 10 to Fig. 3a). Moreover, as is shown in Fig. 11, the vertical resolution increase has the largest impact at high horizontal resolution, whereas the low horizontal resolution simulations are hardly affected by the vertical resolution increase (cf. Fig. 11a-e with Fig. 11f). That the near convergence in the mid- to lower stratosphere for medium-range forecasts is achieved at 200m (or L198) vertical resolution at TCo1279 horizontal resolution can be seen by comparing panel d) to panels a-c) in Fig. 11.

Examination of the eddy kinetic energy spectrum between high and low vertical resolution forecasts at TCo1279 horizontal resolution, reveals that the high vertical resolution forecasts have more energy in total wavenumbers  $N > 50$  in the stratosphere, than their low vertical resolution counterparts (cf. thin blue line to thin green line in Fig. 7). An increase in divergent kinetic energy in the stratosphere with increase in vertical resolution has also recently been reported in the Met Office UM by Cullen (2017).

Interestingly, the vertical resolution requirement for convergence in the mid- to lower stratosphere in SEAS5 is also 200m (compare green and pink lines at L198 vertical resolution to grey lines at L320 vertical resolution in Fig. 2), despite the much lower horizontal resolution in SEAS5 than in medium-range forecasts (i.e., TCo199 and TCo319 vs TCo1279). It is possible that for longer lead times than 10 days, the TCo1279 forecasts would continue to cool more than the lower horizontal resolution forecasts. Therefore, vertical grid spacing finer than 200m in the mid- to lower stratosphere might be required to alleviate horizontal resolution sensitivity of temperature at longer lead time.

However, it is also possible that the vertical resolution requirement for alleviating the global-mean cooling problem in the stratosphere is determined by the amplitude of gravity wave energy (i.e., the divergent kinetic energy spectrum) in total wavenumbers  $40 < N < 300$ , as these horizontal scales appear to produce 1-3km vertical scales that require high vertical resolution. As the divergent eddy kinetic energy in horizontal wavenumbers  $40 < N < 300$  is similar for horizontal resolutions  $> \text{TCo399}$  (cf. red to blue thin line in Fig. 7), similar vertical resolution requirement is likely for all horizontal resolutions larger than TCo399.

### 3.3 Higher order vertical interpolation

The increase in the vertical resolution ultimately results in a more accurate vertical advection. Therefore, the next natural question to ask is whether an implementation of a higher order vertical interpolation in the semi-Lagrangian dynamical core could help to alleviate the global-mean cooling observed when increasing the horizontal resolution. In the current operational IFS (at the time of writing, CY46R1), a third-order Lagrange interpolation is used to interpolate prognostic variables to the trajectory departure point in the horizontal and vertical directions. To test if higher order vertical interpolation is of benefit to the cooling problem, forecasts with a quintic Lagrange vertical interpolation, applied on temperature and specific humidity are performed<sup>4</sup>.

Figure 12 shows that the quintic vertical interpolation indeed reduces the horizontal resolution sensitivity (Fig. 12a vs Fig. 12b) by warming the higher horizontal resolution forecasts (Fig. 12c vs Fig. 12d).

<sup>4</sup>Quintic vertical interpolation on specific humidity is applied for consistency. Further tests indicate that quintic vertical interpolation on specific humidity only results in very little change from cubic interpolation.

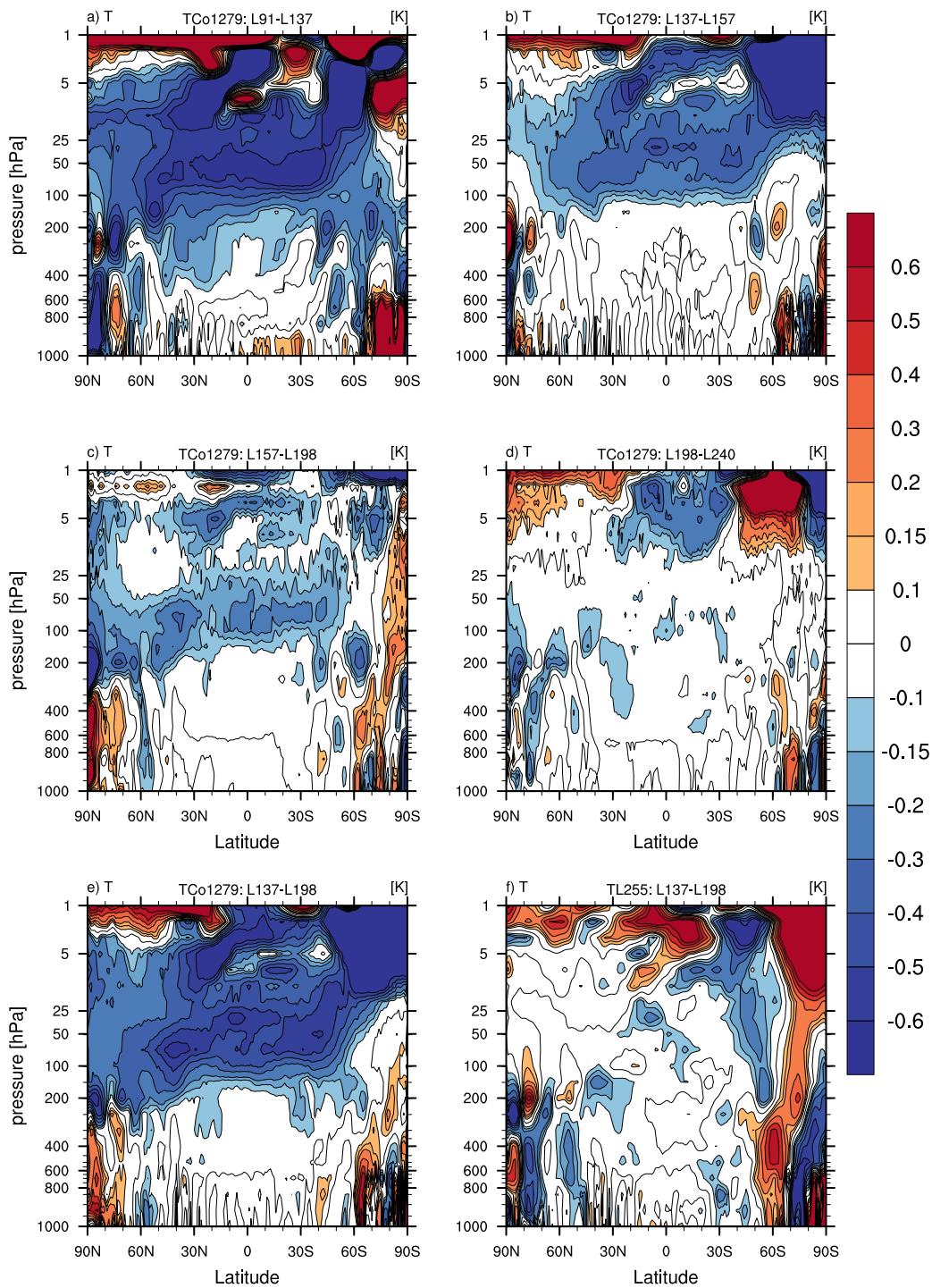


Figure 11: Latitude-pressure cross sections of the zonal-mean temperature difference between lower and higher vertical resolutions at (a-e) TCo1279 horizontal resolution, and, (f) TL255 horizontal resolution. (a) L91 - L137; (b) L137-L158; (c) L158-L198; (d) L240-L198; (e) L137-L198 (TCo1279); (f) L137-L198 (TL255). Note the larger impact of vertical resolution increase at high horizontal resolution.

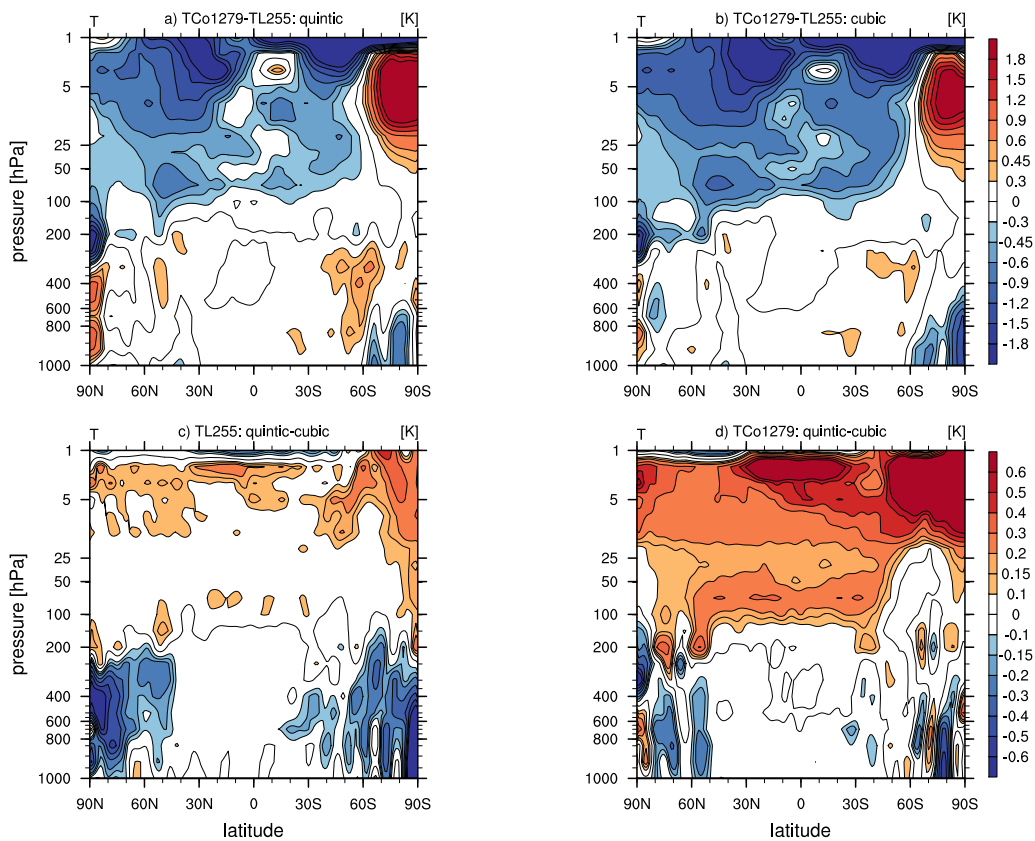


Figure 12: (a-b): Latitude-pressure cross sections of the zonal-mean temperature difference between TCo1279 and TL255 for (a) quintic, and, (b) cubic vertical interpolation. (c-d) Difference in zonal-mean temperature between quintic and cubic at (c) TL255 horizontal resolution, and, (d) TCo1279 horizontal resolution. Panel (b) in this figure is a repeat of Fig. 3a. Note the larger impact of quintic interpolation at high horizontal resolution. Note also the reduction in horizontal resolution sensitivity with quintic interpolation.

### 3.4 Filtering grid-scale oscillations in the vertical

Both increasing the vertical resolution or implementing a higher-order vertical semi-Lagrangian interpolation reduce the global-mean stratospheric cooling observed when horizontal resolution is increased. This confirms that the problem arises from the discretization errors in the representation of vertical advection. It is therefore of interest to establish if filtering grid-scale oscillations in the vertical direction will also result in alleviating the ‘cooling with increase in horizontal resolution’ problem by essentially eliminating these poorly resolved waves. To test this, a Laplacian vertical grid-point filter in the semi-Lagrangian interpolation (SLVF, described in Váňa et al. (2008)), that most strongly damps  $2\Delta z$  grid scale oscillations, was applied throughout the vertical domain on temperature only, leaving the horizontal direction unfiltered. Thus unlike the strong divergence damping (i.e., the “deep sponge”) setup, the SLVF filter does not damp energy in horizontal wavenumbers (this was verified by calculating the kinetic energy spectrum with the SLVF filter on). As the SLVF filters oscillations that are unresolved in the vertical direction, it does not damp energy/momentum fluxes for gravity waves with larger vertical wavelengths ( $>2\text{km}$ ) and horizontal wavelengths in the  $40 < N < 300$  total wavenumber range. It should be noted that while the SLVF filter damps the  $2\Delta z$  oscillations the strongest, it also damps oscillations  $> 2\Delta z$ .

Figure 13 shows the impact of the SLVF filter on the zonal-mean temperature. Clearly, the vertical filtering is beneficial for the cooling problem, as the horizontal resolution sensitivity almost disappears in the lower- to mid- stratosphere when the filter is applied (cf. Fig. 13a with Fig. 3a). Again, the impact of the filter is felt more strongly in the high horizontal resolution forecasts (cf. Fig. 13b with Fig. 13c), confirming that the dynamical core is struggling to accurately represent gravity wave propagation in the vertical in the stratosphere, if the vertical resolution/aspect ratio is not fine enough.

## 4 Impact on medium-range forecast skill scores

Having established that a higher vertical resolution, quintic vertical interpolation, and the SLVF vertical filter, all alleviate the global-mean cooling observed when increasing horizontal resolution, it is timely to examine the impact of these model changes on medium-range forecast skill scores. In what follows, testing is done in forecast mode only and all forecasts are verified against the HRES operational analysis. For more accurate verification, analysis experiments with these model changes need to be performed.

Figures 14-16 show the impact of increased vertical resolution on the root-mean square error of geopotential height (henceforth Z RMSE) at different lead times, at TCo1279 horizontal resolution. It is clear that the lower- to mid- stratospheric Z RMSE is improved by as much as 50% in the 240L vertical resolution experiments. This improvement is coming from the improvement in the zonal-mean temperature in the lower- to mid- stratosphere, as shown in Fig. 17. Thus, increased vertical resolution indeed reduces the global-mean cooling of the stratosphere, leading to a reduction of the cold bias in the lower- to mid-stratosphere, but an increase of the the warm bias in the upper stratosphere, at least when verified against HRES operational analysis.

Figures 18-20 show the impact of the quintic vertical interpolation on the Z RMSE and on the regional mean temperature error in the stratosphere. Again, the impact of the quintic vertical interpolation is positive in the lower- to mid- stratosphere but negative in the upper stratosphere, for exactly the same reason as for the higher vertical resolution forecasts. In addition, skill score improvement from quintic vertical interpolation and a moderate vertical level increase (to 300m or 157L) appears to be additive. This is shown in Figs. 19-20. For example, Fig. 20 shows that the TCo1279L157 quintic vertical interpolation

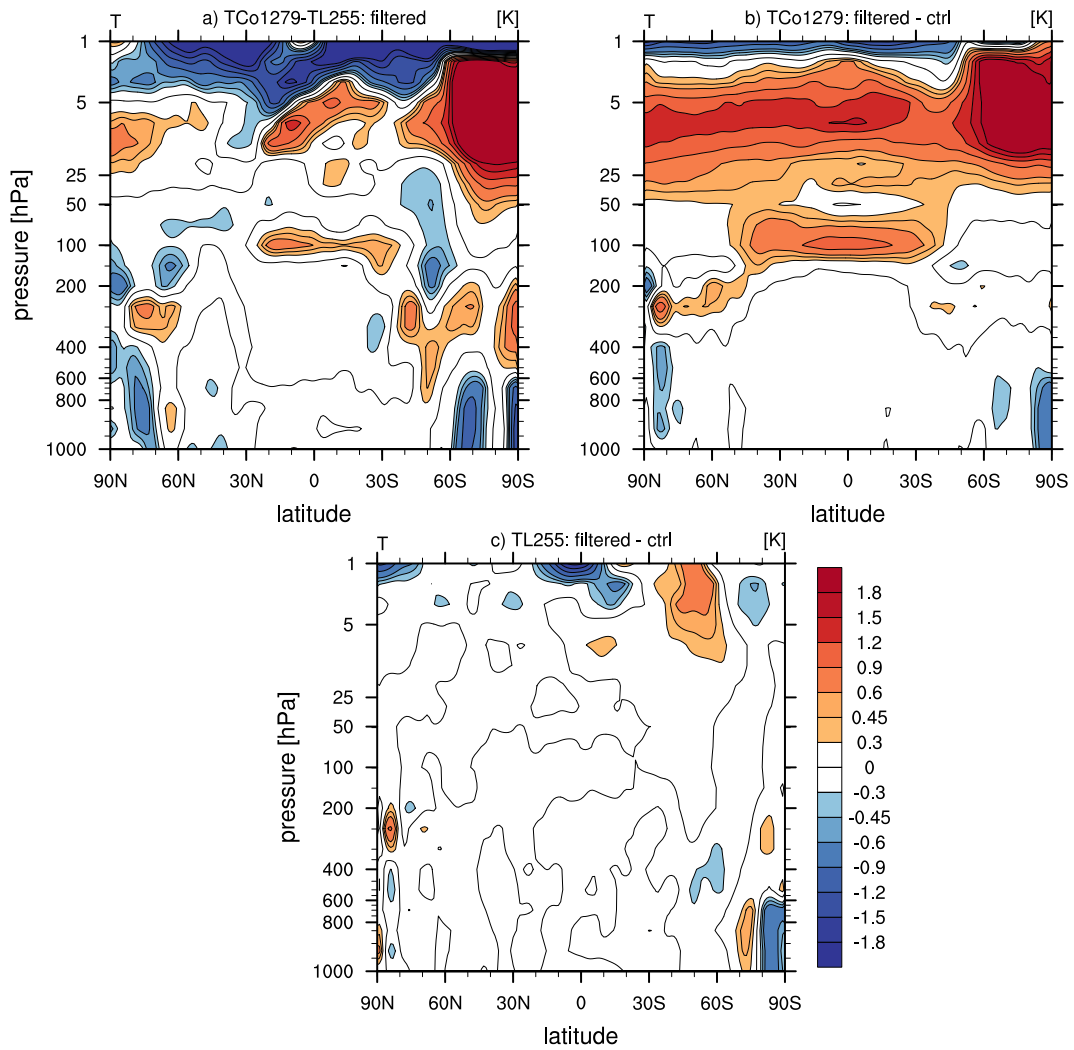


Figure 13: (a): Latitude-pressure cross sections of the zonal-mean temperature difference between TCo1279L137 and TL255L137 for forecasts with the SLVF vertical grid point filter applied on temperature. (b) Difference in temperature between filtered and unfiltered forecasts at TCo1279L137. (c) Same as (b), but at TL255L137 resolution. The filter strength is SLHDEPSV=0.0025.

forecast (green lines) show less cooling at 50 hPa than the TCo1279L157 cubic vertical interpolation forecast (black lines) and TCo1279L137 quintic vertical interpolation forecast (red lines).

Finally, the impact of vertical SLVF filter on the Z RMSE and on the regional mean temperature error in the stratosphere is shown in Figs. 21-22. As expected, the impact of the SLVF filter is positive in the lower- to mid stratosphere. Moreover, the horizontal resolution sensitivity of the temperature drift is reduced by the use of the SLVF filter (cf. red and green lines at TCo1279 horizontal resolution to black and blue lines at TCo399 horizontal resolution). However, more tuning to the SLVF filter would be required (e.g., to the filter coefficient or to the vertical extent over which SLVF is applied) for better performance, especially in the tropical troposphere (see the negative RMSE signal there in Fig. 21).

## 5 Summary, conclusions and recommendations

The global-mean cooling observed in the IFS when the horizontal resolution is increased is due to the dynamical core. This cooling exacerbates the lower- to mid stratospheric cold bias and makes the model development hard (as e.g. model tuning performed at lower horizontal resolution might no longer be valid at higher horizontal resolution). Several causes for the global-mean cooling were investigated and it was shown that it arises from discretization errors in vertical advection. That the cooling with horizontal resolution increase is unphysical was further illustrated by a dry idealized flow over topography test case, devoid of any sources or sinks, where it was shown that the IFS experiences a larger loss of global-mean temperature at higher horizontal resolution.

As the horizontal resolution increases, a larger part of the gravity wave spectrum is resolved in the horizontal. However, resolving vertical propagation of such gravity waves — especially in the stratosphere — is a challenge at operational vertical resolutions (L137 for HRES, L91 for ENS and SEAS5). It was shown that increasing the vertical resolution sufficiently to resolve 1-3km vertical wavelength waves in the lower- to mid stratosphere alleviated the global-mean cooling at high horizontal resolution. Improving the accuracy of vertical advection via a quintic vertical interpolation (instead of a cubic) was also shown to be able to contribute to an alleviation of the cooling at high horizontal resolution. Moreover, if the poorly resolved 1-3km vertical wavelength waves were filtered out in the temperature field in the vertical direction, the cooling at high horizontal resolution disappeared. Thus the solution is to either resolve the 1-3km vertical wavelengths well (via an increase in vertical resolution or quintic vertical interpolation) or not have them in the model at all (via filtering them out in the vertical).

These results have following implications:

- The horizontal wavelengths responsible for the undesired cooling at higher horizontal resolution are  $\mathcal{O}(50 - 500\text{km})$ . Such waves are well resolved at TCo1279 horizontal resolution. If the kinetic energy in these horizontal wavelengths is unchanged as a result of further increase in horizontal resolution, it is unlikely that the cooling problem will be exacerbated at higher resolution than TCo1279. Indeed, a comparison of kinetic energy spectrum at TCo2559 and TCo1279 horizontal resolutions shows an equal amount of energy in total wavenumbers  $40 < N < 300$  (not shown). However, TCo2559 simulations with deep convection parametrization turned off suggest a substantial increase in the amplitude and spectral slope in the  $40 < N < 300$  range (not shown). That the removal of physical parameterizations substantially alters energy spectrum was discussed in [Malardel & Wedi \(2016\)](#). As a result, it is possible that an increase in horizontal resolution accompanied by a removal of parametrized processes could lead to further cooling.
- Horizontal wavelengths in the total wavenumber  $40 < N < 300$  range appear to be associated

with 1-3km vertical wavelengths in the stratosphere. This conclusion is supported by the lower-stratospheric radar observations in [Sato \(1994\)](#), who found that the 100-1000 km horizontal wavelength waves are associated with 1-3km vertical wavelength waves (see Figure 7 and 8 in [Sato \(1994\)](#)). Therefore, the here found 200m (or L198) vertical resolution requirement in the stratosphere is expected from the requirement to resolve 1-3km vertical wavelength waves by  $> 4$  grid points. Therefore any atmospheric model that resolves  $\mathcal{O}(50 - 500\text{km})$  horizontal wavelengths well, would benefit from a vertical resolution increase in the stratosphere that would allow to resolve 1-3km in the vertical.

- It is, however, unclear what role these short 1-3km vertical wavelength waves play in the middle-atmosphere. From the mid-frequency approximation to the gravity wave dispersion relation, the total vertical flux of horizontal momentum due to gravity waves  $F_{\text{ph}}$  is ([Ern et al. 2004](#))

$$F_{\text{ph}} = \frac{1}{2} \bar{\rho} \frac{k_h}{m} \left( \frac{g}{N} \right)^2 \left( \frac{\bar{T}}{T'} \right)^2. \quad (9)$$

Therefore small vertical wavelength waves carry less momentum than large scale waves for a fixed horizontal wavelength. Therefore they are unlikely to play a big role in the momentum budget. This begs a question whether applying a vertical grid point filter (such as SLVF) to remove these small-scale waves would be justified, and, in fact desirable.

- Increasing vertical resolution in the stratosphere is shown to increase gravity wave activity there (see Fig. 7) as the waves propagating from the troposphere into the stratosphere are no longer filtered out by the stretched vertical grid in the UTLS. If the same high vertical resolution is not kept throughout the stratosphere all the way to the start of the sponge, it is possible that the global-mean cooling with horizontal resolution increase is pushed further up. An indication of this can be seen in Fig. 25b, for the idealized gravity wave propagation test case.
- It has been reported in several previous technical memoranda ([Polichtchouk et al. 2017](#), [Hogan et al. 2017](#), [Shepherd et al. 2018](#)) that the removal of the sponge, used to absorb vertically propagating waves near the model top, has a global cooling effect in the upper stratosphere/mesosphere. This result was puzzling and could not be explained via an increase of resolved gravity wave drag and a concomitant strengthening of the residual mean meridional circulation, brought about by the removal of the sponge. This is because any change in upwelling should be compensated by the same change in downwelling, resulting in net zero change in global-mean temperature. Given the results in this study, the answer to this puzzle becomes clearer: The removal of the sponge leads to more energy in  $40 < N < 300$  waves in the upper stratosphere/mesosphere, and, therefore to more unresolved vertical grid-scale oscillations. This, in turn, implies more discretization errors in the vertical advection and hence stronger global mean cooling. However, with an increase of vertical resolution to 200 m throughout the middle atmosphere, the global warming effect of the sponge is likely to disappear.
- The above point should be contrasted with the result that by removing the sponge, gravity wave momentum fluxes are closer to the observations (e.g. lidar observations in Scandinavia and Patagonia – [Gissinger et al. manuscript in preparation](#)). Therefore, while the sponge might reduce the global-mean cooling problem (at the current vertical resolution) by filtering out all gravity waves, it damps the well resolved (in both the horizontal and vertical directions) gravity wave momentum fluxes too much. Note that short vertical wavelength waves are not expected to carry much momentum (see third point above). Therefore, a potential model improvement would be to filter out unresolved gravity waves in the vertical by the SLVF filter while reducing the depth of the sponge.

The SLVF filter would alleviate the unwanted global-mean cooling, while a shallower sponge would improve the amplitude of resolved gravity wave momentum fluxes in the stratosphere.

- Finally, this report highlights an important point for model development in that any dynamical core changes, which affect the middle atmosphere, need to be tested at high horizontal resolution. As seen here, erroneous conclusions of “no-impact” might be drawn if tests are only conducted at low horizontal resolution.

The recommendations from these findings are as follows:

- Given the temperature sensitivity to the vertical resolution, all forecasting systems (i.e., HRES, ENS and SEAS5) should employ the same vertical resolution in order to make model development easier.
- More accurate quintic vertical interpolation on temperature and specific humidity should be used operationally, as this reduces the horizontal resolution sensitivity in the stratosphere.
- To further alleviate the horizontal resolution sensitivity and improve skill scores in the lower- to mid- stratosphere, a possibility of combining quintic vertical interpolation with the SLVF filter should be further explored as this is a cheaper alternative to increase in vertical resolution. This could allow for the implementation of modified solar UV spectrum in the radiation scheme discussed in [Hogan et al. \(2017\)](#). While 300m (i.e., L157) vertical resolution accompanied with the quintic vertical interpolation would already greatly improve on the horizontal resolution sensitivity, the cost of vertical resolution increase can not be at present justified given the lack of skill improvement in the troposphere.
- Ultimately, consideration should be given to an increase in the vertical resolution everywhere in the stratosphere all the way up to the model sponge. Stretching in the vertical grid in the stratosphere before the model sponge should be avoided. However, more work is needed to assess the impact of better gravity wave representation in the stratosphere on tropospheric forecast skill. Thus far, medium- and extended-range forecasts with higher vertical resolution have not shown enhanced tropospheric predictability.

## Acknowledgments

The authors thank Thomas Birner, Mike Blackburn, Almut Gassmann and Ted Shepherd for helpful discussions on the topic.

## References

- Andrews, D. G., Holton, J. R. & Leovy, C. B. (1987), *Middle atmosphere dynamics*, number 40, Academic press.
- Bacmeister, J. T., Eckermann, S. D., Newman, P. A., Lait, L., Chan, K. R., Loewenstein, M., Proffitt, M. H. & Gary, B. L. (1996), ‘Stratospheric horizontal wavenumber spectra of winds, potential temperature, and atmospheric tracers observed by high-altitude aircraft’, *Journal of Geophysical Research: Atmospheres* **101**(D5), 9441–9470.

- Becker, E. (2003), 'Frictional heating in global climate models', *Monthly Weather Review* **131**(3), 508–520.
- Billant, P. & Chomaz, J.-M. (2001), 'Self-similarity of strongly stratified inviscid flows', *Physics of Fluids* **13**(6), 1645–1651.
- Birner, T., Sankey, D. & Shepherd, T. G. (2006), 'The tropopause inversion layer in models and analyses', *Geophysical Research Letters* **33**(14).
- Burgess, B. H., Erler, A. R. & Shepherd, T. G. (2013), 'The troposphere-to-stratosphere transition in kinetic energy spectra and nonlinear spectral fluxes as seen in ecmwf analyses', *Journal of the Atmospheric Sciences* **70**(2), 669–687.
- Cullen, M. J. P. (2017), 'The impact of high vertical resolution in the met office unified model', *Quarterly Journal of the Royal Meteorological Society* **143**(702), 278–287.
- Ern, M., Preusse, P., Alexander, M. J. & Warner, C. D. (2004), 'Absolute values of gravity wave momentum flux derived from satellite data', *Journal of Geophysical Research: Atmospheres* **109**(D20).
- Fritts, D. C. & Alexander, M. J. (2003), 'Gravity wave dynamics and effects in the middle atmosphere', *Reviews of Geophysics* **41**(1).
- Fueglistaler, S., Haynes, P. H. & Forster, P. M. (2011), 'The annual cycle in lower stratospheric temperatures revisited', *Atmospheric Chemistry and Physics* **11**(8), 3701–3711.  
**URL:** <https://www.atmos-chem-phys.net/11/3701/2011/>
- Haynes, P., McIntyre, M., Shepherd, T., Marks, C. & Shine, K. P. (1991), 'On the “downward control” of extratropical diabatic circulations by eddy-induced mean zonal forces', *Journal of the Atmospheric Sciences* **48**(4), 651–678.
- Hogan, R., Ahlgrimm, M., Balsamo, G., Beljaars, A., Berrisford, P., Bozzo, A., Giuseppe, F. D., Forbes, R., Haiden, T., Lang, S., Mayer, M., Polichtchouk, I., Sandu, I., Vitart, F. & Wedi, N. (2017), 'Radiation in numerical weather prediction', *ECMWF Technical Memorandum* (816).
- Lindzen, R. S. & Fox-Rabinovitz, M. (1989), 'Consistent vertical and horizontal resolution', *Monthly Weather Review* **117**(11), 2575–2583.
- Malardel, S. & Wedi, N. P. (2016), 'How does subgrid-scale parametrization influence nonlinear spectral energy fluxes in global nwp models?', *Journal of Geophysical Research: Atmospheres* **121**(10), 5395–5410.
- Nastrom, G. D. & Gage, K. S. (1985), 'A climatology of atmospheric wavenumber spectra of wind and temperature observed by commercial aircraft', *Journal of the Atmospheric Sciences* **42**(9), 950–960.
- Plumb, R. A. (2002), 'Stratospheric transport', *Journal of the Meteorological Society of Japan. Ser. II* **80**(4B), 793–809.
- Polichtchouk, I., Hogan, R., Shepherd, T., Bechtold, P., Stockdale, T., Malardel, S., Lock, S.-J. & Magnusson, L. (2017), 'What influences the middle atmosphere circulation in the ifs?', *ECMWF Technical Memorandum* (809).
- Sato, K. (1994), 'A statistical study of the structure, saturation and sources of inertio-gravity waves in the lower stratosphere observed with the mu radar', *Journal of atmospheric and terrestrial physics* **56**(6), 755–774.

- Shepherd, T., Polichtchouk, I., Hogan, R. & Simmons, A. (2018), ‘Report on stratosphere task force’, *ECMWF Technical Memorandum* (824).
- Ullrich, P. A., Jablonowski, C., Reed, K. A., Zarzycki, C., Lauritzen, P. H., Nair, R. D., Kent, J. & Verlet-Banide, A. (2016), ‘Dynamical core model intercomparison project (dcmip2016) test case document’, URL <https://github.com/ClimateGlobalChange/DCMIP2016>.
- Untch, A. & Hortal, M. (2004), ‘A finite-element scheme for the vertical discretization of the semi-lagrangian version of the ecmwf forecast model’, *Quarterly Journal of the Royal Meteorological Society* **130**(599), 1505–1530.
- Váňa, F., Bénard, P., Geleyn, J.-F., Simon, A. & Seity, Y. (2008), ‘Semi-lagrangian advection scheme with controlled damping: An alternative to nonlinear horizontal diffusion in a numerical weather prediction model’, *Quarterly Journal of the Royal Meteorological Society: A journal of the atmospheric sciences, applied meteorology and physical oceanography* **134**(631), 523–537.
- Waite, M. L. (2016), ‘Dependence of model energy spectra on vertical resolution’, *Monthly Weather Review* **144**(4), 1407–1421.
- Waite, M. L. & Bartello, P. (2004), ‘Stratified turbulence dominated by vortical motion’, *Journal of Fluid Mechanics* **517**, 281308.
- Wedi, N. P. & Smolarkiewicz, P. K. (2006), ‘Direct numerical simulation of the plumbmcewan laboratory analog of the qbo’, *Journal of the Atmospheric Sciences* **63**(12), 3226–3252.
- Wedi, N. P. & Smolarkiewicz, P. K. (2009), ‘A framework for testing global non-hydrostatic models’, *Quarterly Journal of the Royal Meteorological Society* **135**(639), 469–484.

## A Idealized gravity wave propagation test case

It is shown here that the global mean cooling observed when the horizontal resolution is increased can also be seen in a very idealized dry “gravity wave propagation” test case, devoid of sources or sinks.

The setup is a “uniform flow over a Gaussian mountain” test case on a small planet. The details of the setup can be found in [Ullrich et al. \(2016\)](#) and are summarized in a schematic in [Fig 23](#). Essentially, the initial condition is isothermal atmosphere with uniform  $10 \text{ m s}^{-1}$  zonal wind. A Gaussian mountain, with 50km half-width and 2km height is prescribed. In a small-planet setup ([Wedi & Smolarkiewicz 2009](#)), the radius of a planet is reduced, so that the gravity wave generation and propagation can be studied even at a relatively coarse resolution. Horizontal resolution sensitivity is performed at TCo639L91 and TCo319L191 resolutions with identical time step size of  $\Delta t = 75\text{s}$ . The planetary radius is reduced by a factor of 12, so that the half-width of a mountain is resolved by at least 16 grid points. It is important to stress that this test case is free from critical layers, moist dynamics, and, externally imposed sources/sinks. In addition, all explicit numerical filters (including the sponge near the upper boundary) are switched off.

[Figure 24](#) shows temperature perturbation at 24 hours into the evolution, showing a gravity wave propagation with vertical wavelength of 3-4km. [Figure 25](#) shows the difference in global-mean temperature between the high (TCo639) and low (TCo319) horizontal resolutions as a function of pressure and lead time. As expected, the IFS cools more in the global-mean at higher horizontal resolution. Moreover, the

“problem” seems to be unrelated to critical levels. As there are no externally imposed sources/sinks, the vertically integrated global mean temperature should be conserved. However, this is clearly not the case. The drift in vertically averaged global-mean temperature can further be seen in the global temperature norm in Fig. 26.

This idealized test case provides a convenient testbed to assess the impact of other model changes on the global-mean cooling with resolution problem. Thus, the impact of 1) the use of less accurate vertical finite differencing vertical discretization on the Lorenz staggered grid, instead of the operational third order finite element vertical discretization; 2) the vertical resolution increase; and, 3) quintic vertical interpolation is further assessed. The results on the global-mean temperature and the temperature norm are also shown in Figs. 25-26.

As expected, all setups show loss of global-mean temperature, which is exacerbated with increase in horizontal resolution. It is also clear that the third order vertical finite elements perform considerably better than vertical finite differencing (cf. black and dark green curves with red and blue curves in Fig. 26). As is the case for the full model setup, quintic vertical interpolation also improves on the global-mean cooling (cf. cyan and orange curves with red and blue curves in Fig. 26).

Interestingly, there is a lack of obvious improvement in global-mean temperature with increase in vertical resolution (see Fig. 25b, and, cf. light green and pink curves with red and blue curves in Fig. 26). As the vertical resolution is increased, less gravity waves are filtered out as they propagate into the middle atmosphere, resulting in more energy in the divergent modes (see Fig. 7 for the full forecasts). Since the global-mean cooling is associated with inadequate representation of gravity wave propagation by the vertical advection, increasing the vertical resolution in the mid- to lower stratosphere appears to just push the problem from lower down to higher up, as confirmed in Fig. 25b. While in the 100-10hPa region, the increase in vertical resolution alleviates the cooling with increase in horizontal resolution problem, higher up, where the vertical resolution begins to decrease again, the cooling with horizontal resolution re-emerges and is stronger than for the lower vertical resolution experiments (cf. Fig. 25a with Fig. 25b). This would imply that the increase in vertical resolution should be carried out all the way to the start of the model sponge, where gravity waves leading to this problem are removed.

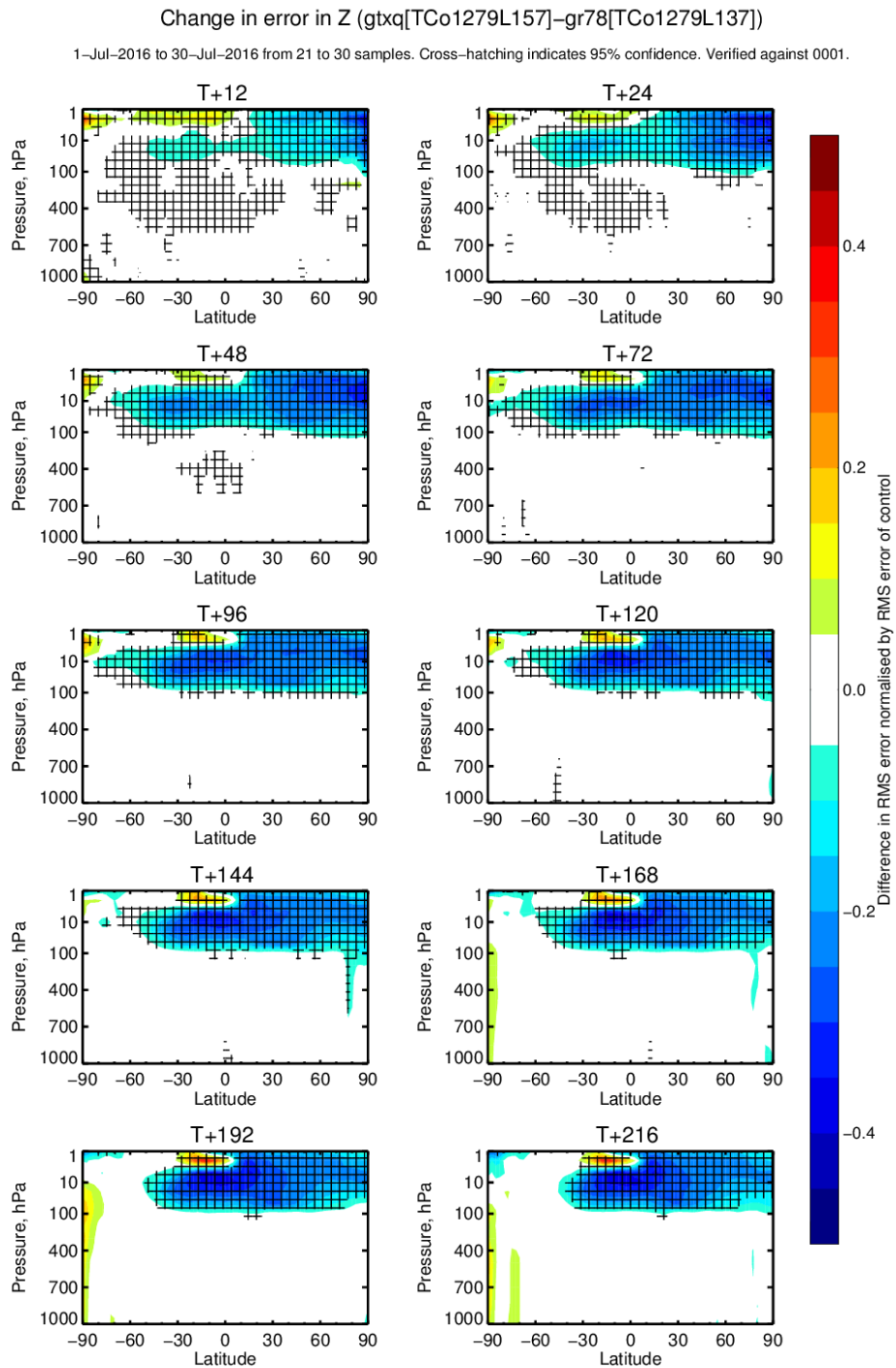


Figure 14: Impact of going to 157 vertical levels from 137 levels on RMSE forecast error of geopotential height for different lead times. Blue colors show that increase vertical resolution lowers (i.e., improves) RMSE. Horizontal resolution is TCo1279. CY43R3. Verification is against HRES operational analysis.

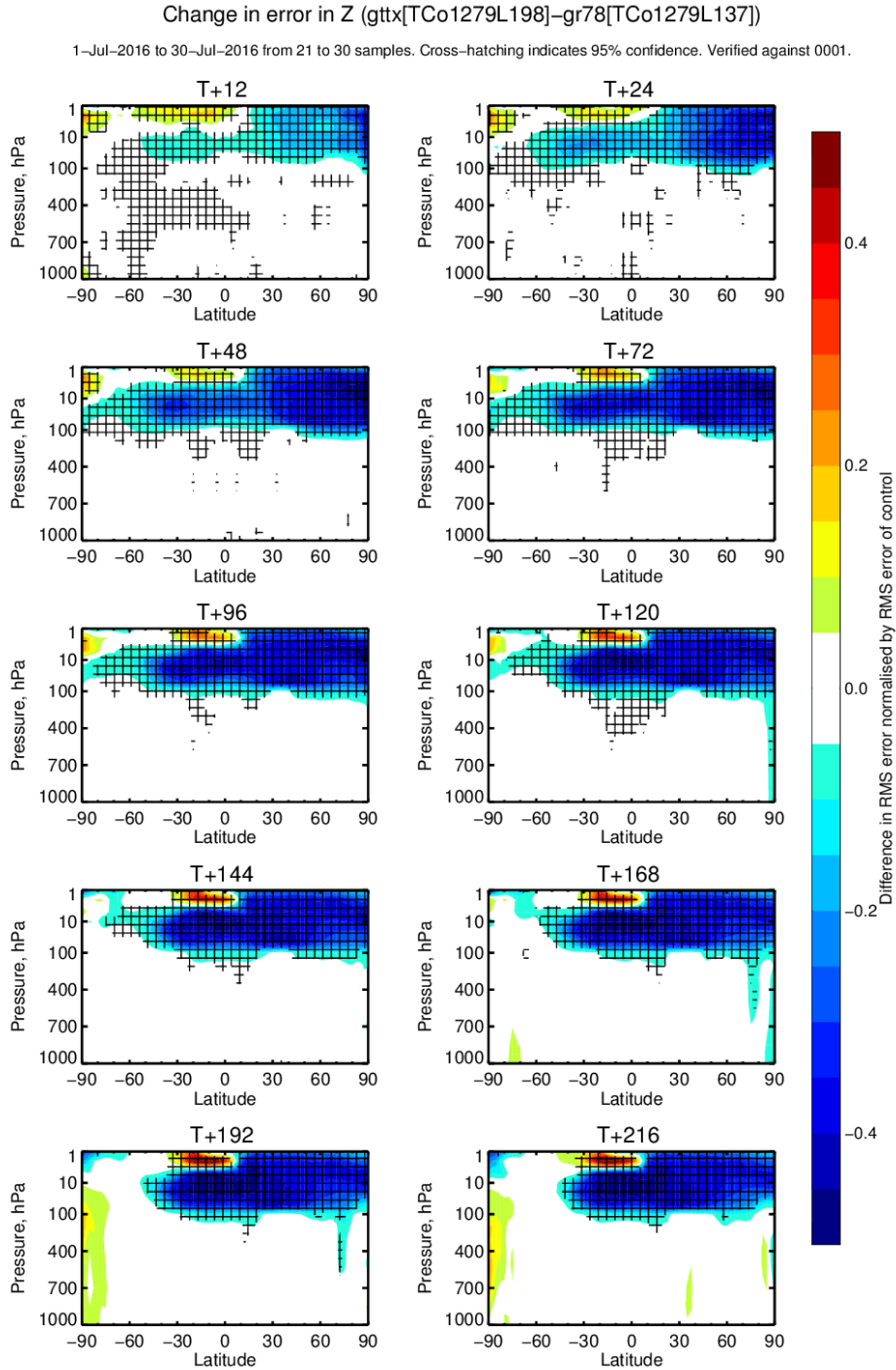
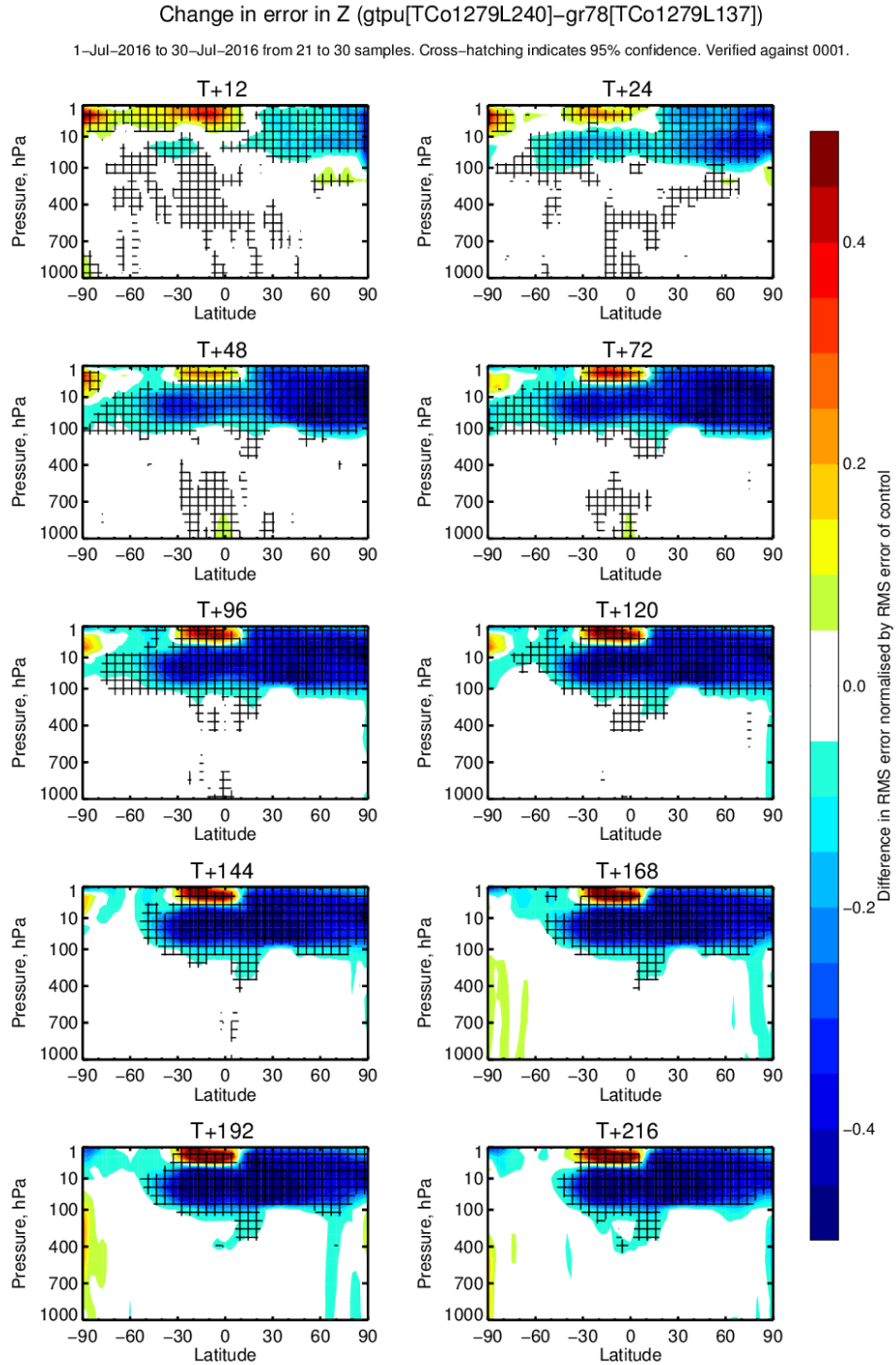


Figure 15: Same as Fig. 14, but for 198 levels.



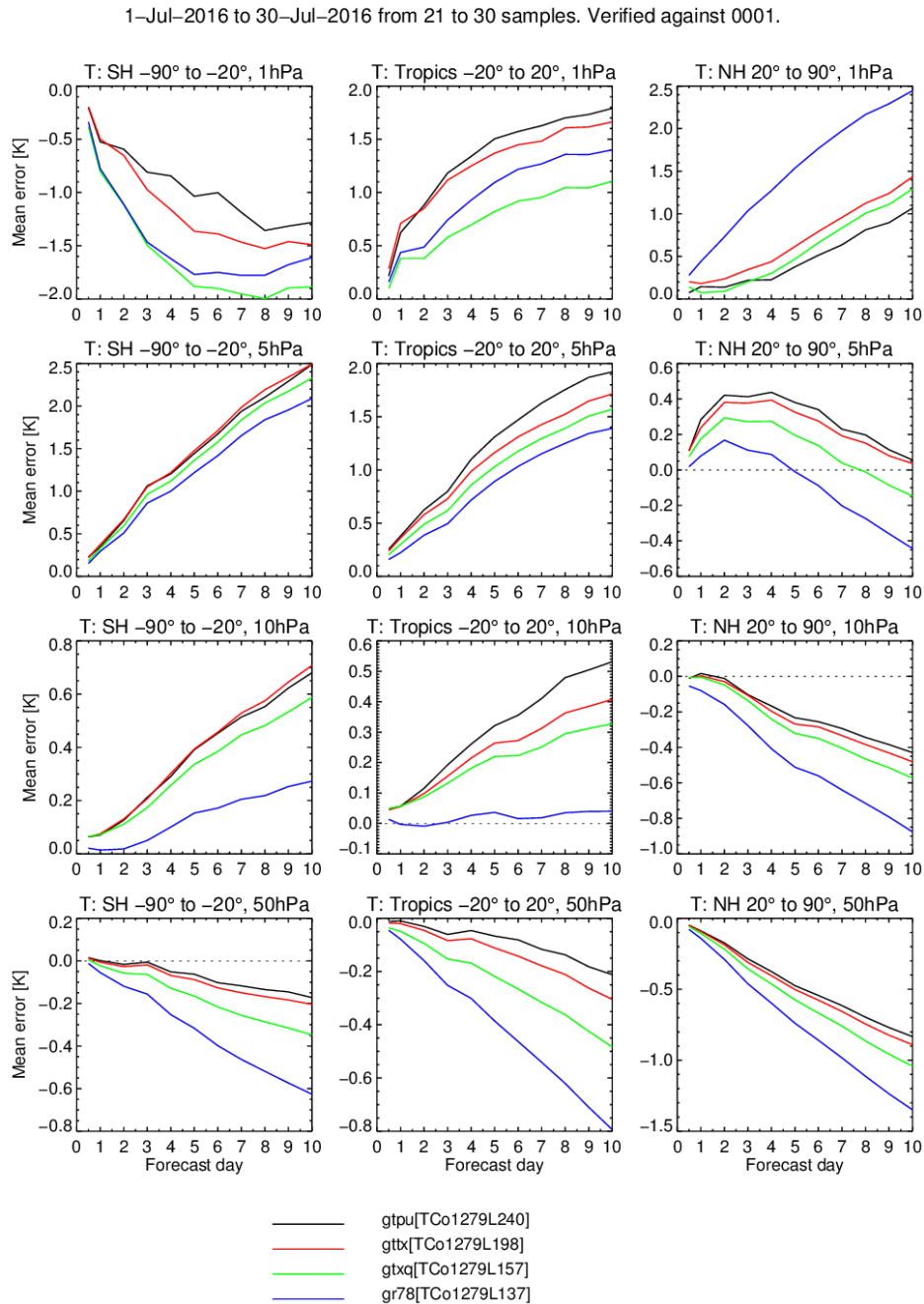


Figure 17: Regional mean temperature error [K] at different heights in the stratosphere for 137L, 157L, 198L and 240L experiments at TCo1279 horizontal resolution for July. Verification is against HRES operational analysis.

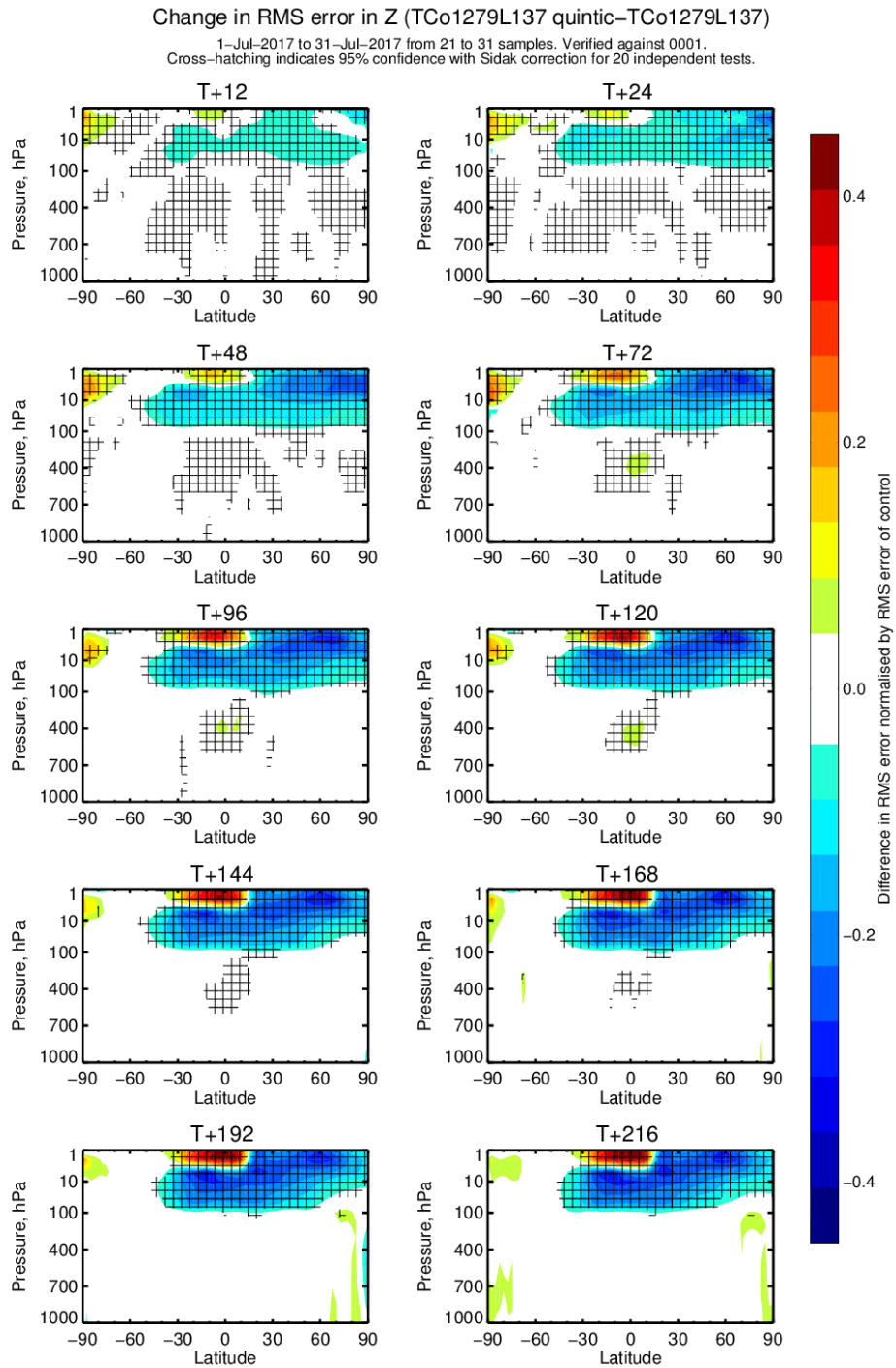


Figure 18: Same as Fig. 14, but for quintic vertical interpolation.

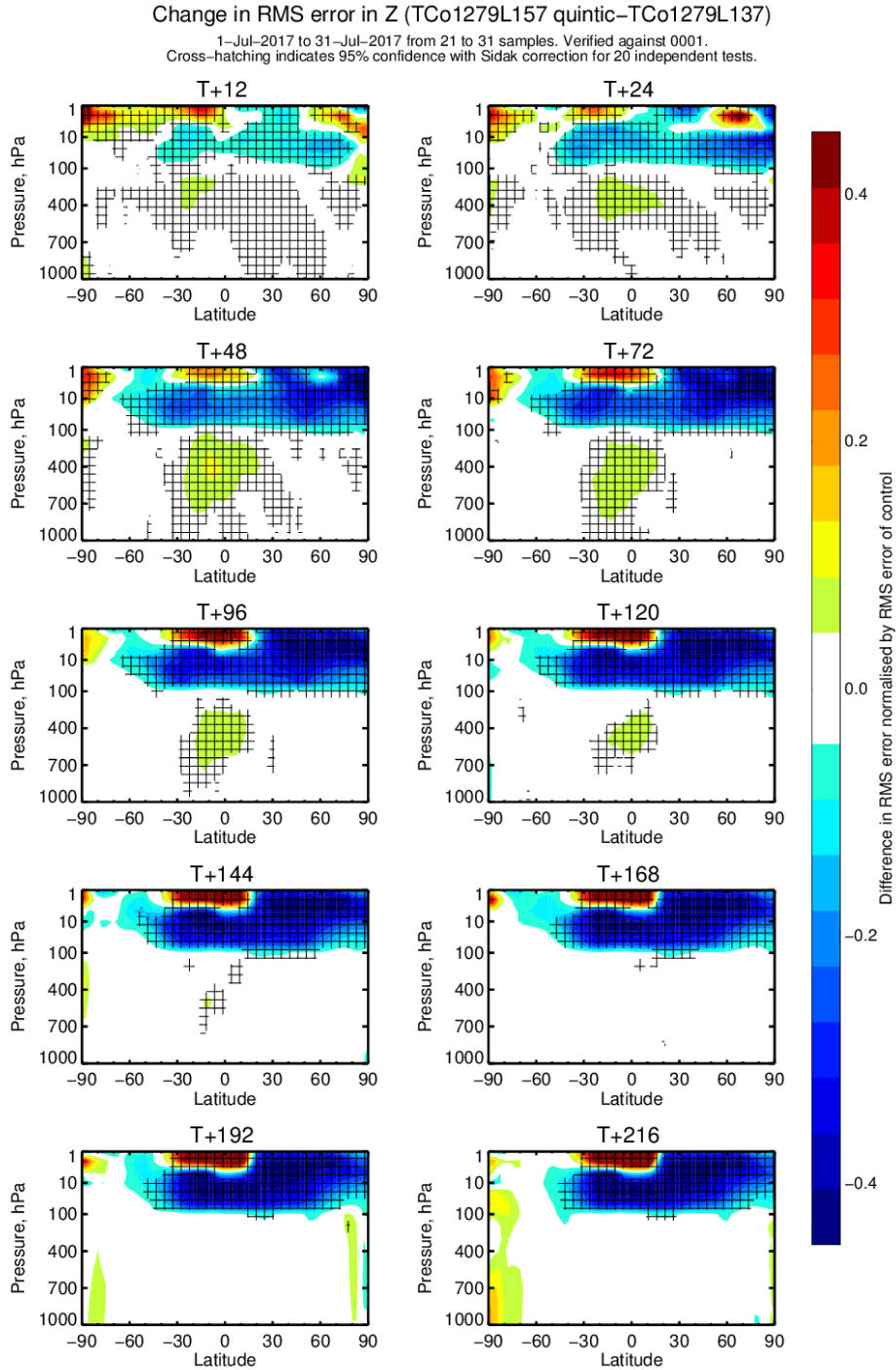


Figure 19: Same as Fig. 14, but for quintic vertical interpolation at 157L vertical resolution.

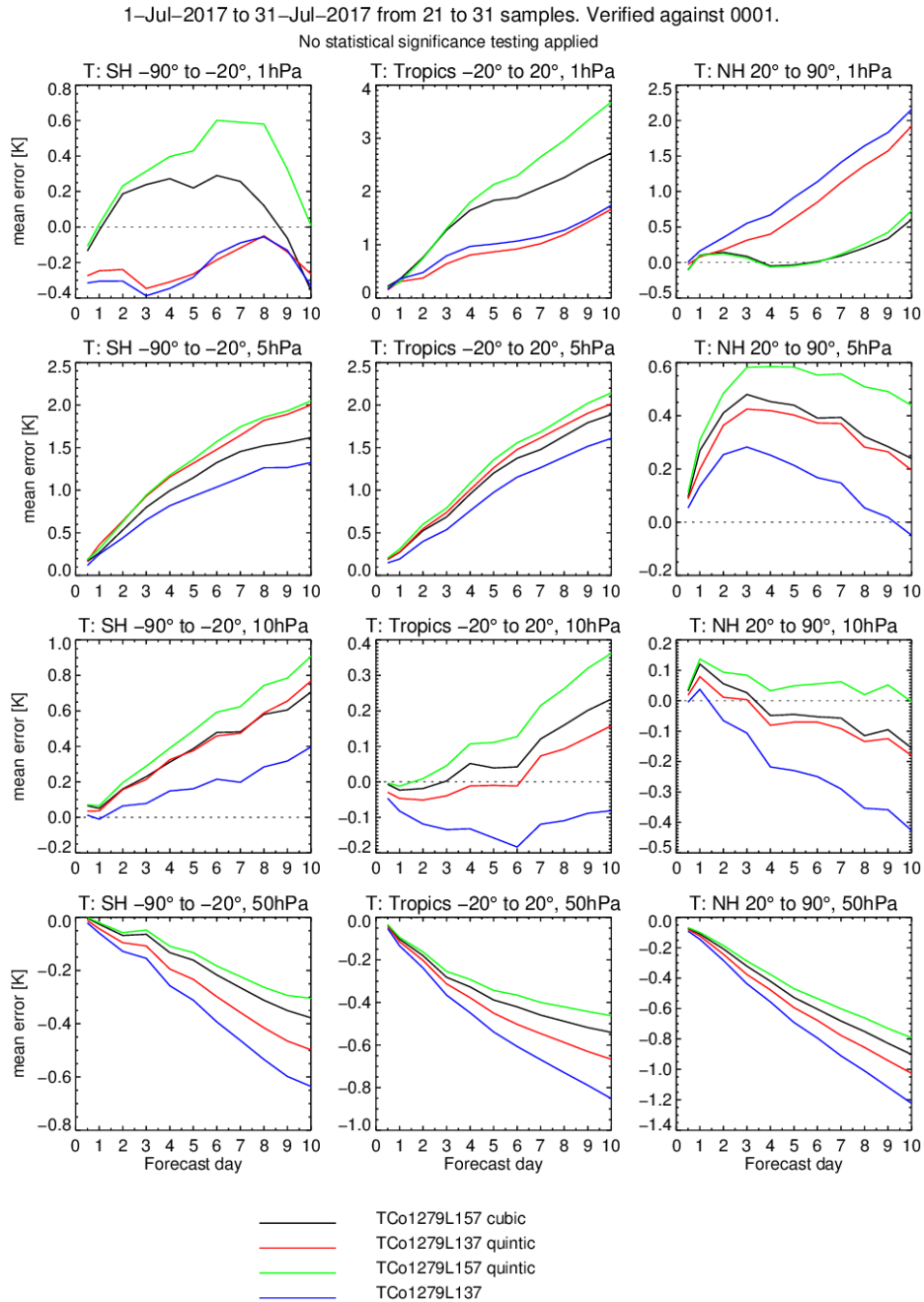


Figure 20: Regional mean temperature error [K] at different heights in the stratosphere for cubic TCo1279L137L, quintic TCo1279L137, cubic TCo1270157L, and, quintic TCo1279L157 forecasts at TCo1279 horizontal resolution for July.

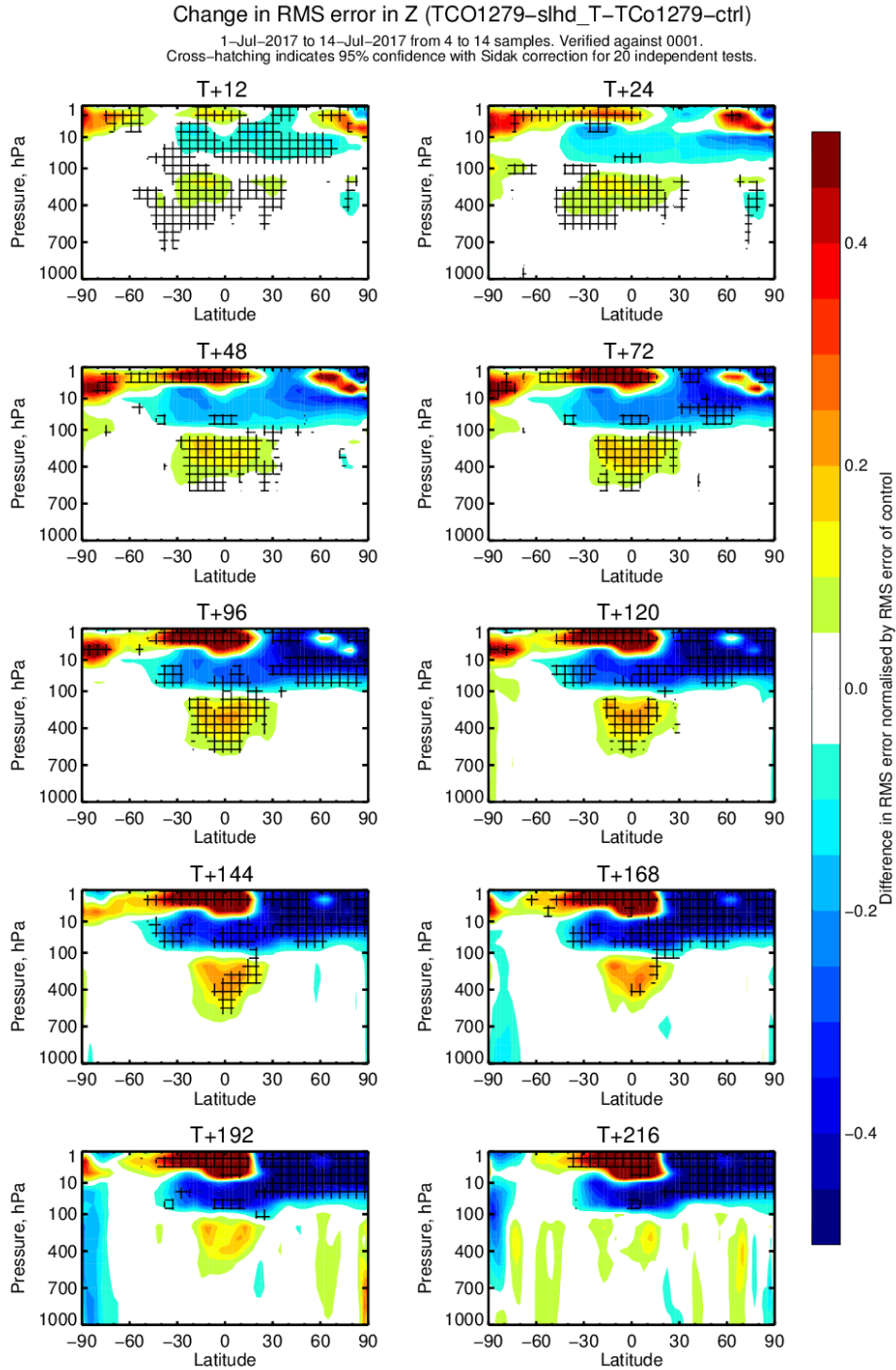


Figure 21: Same as Fig. 14, but for vertical SLVF filter at TCo1279L137 resolution. CY46R1.

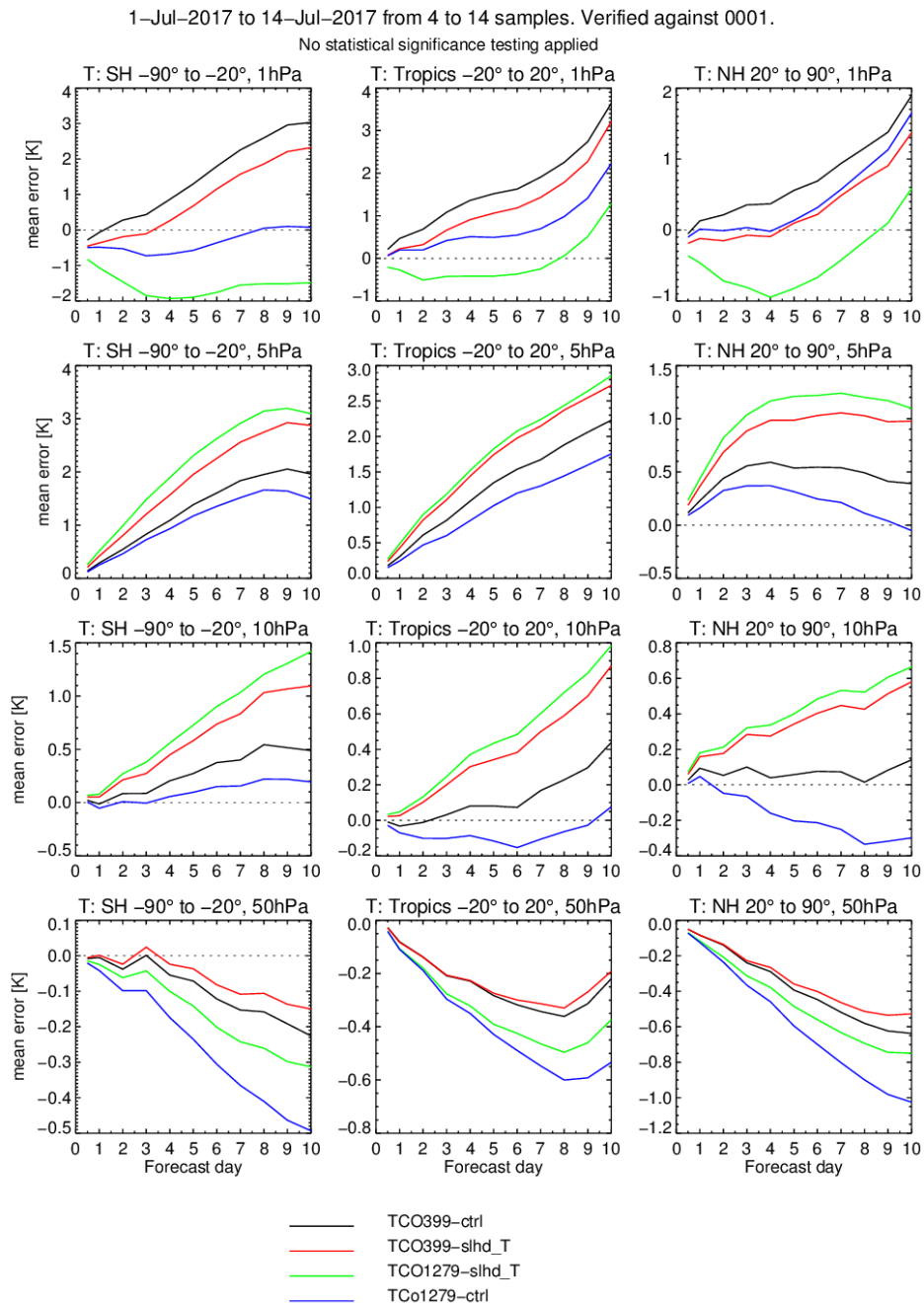


Figure 22: Regional mean temperature error [K] at different heights in the stratosphere for July forecasts with and without SLVF vertical grid point filter at TCo1279L137 (green lines with SLVF, blue lines without) and TCo399L137 (red lines with SLVF, blue lines without) resolutions. July. CY46R1.

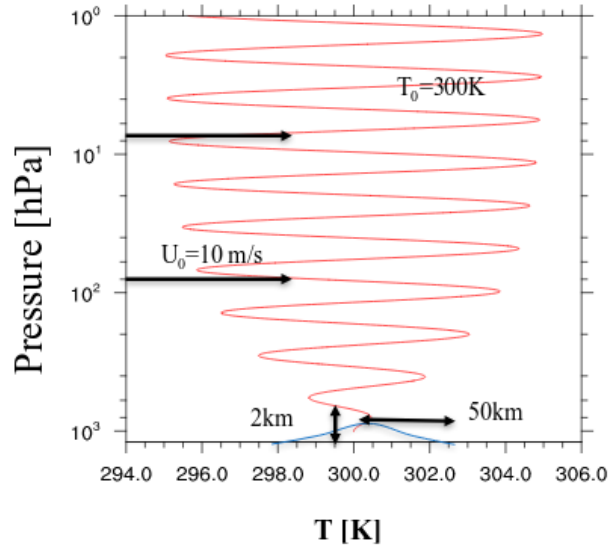


Figure 23: Schematic of the Gaussian mountain test case on a small planet.

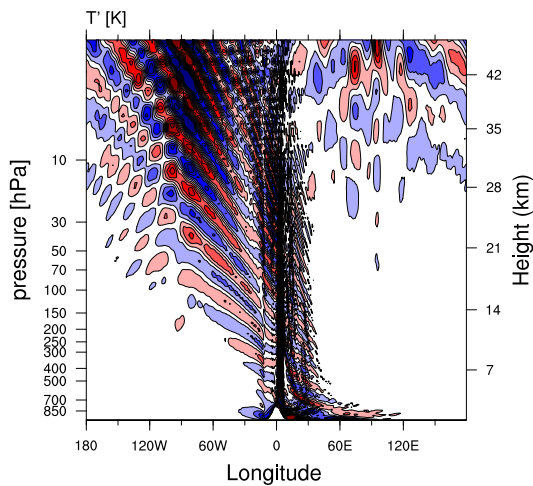


Figure 24: Temperature perturbation [K] (from 300K isothermal reference state) of the Gaussian mountain test case, at  $t=24h$ , at TCo639L137 resolution.

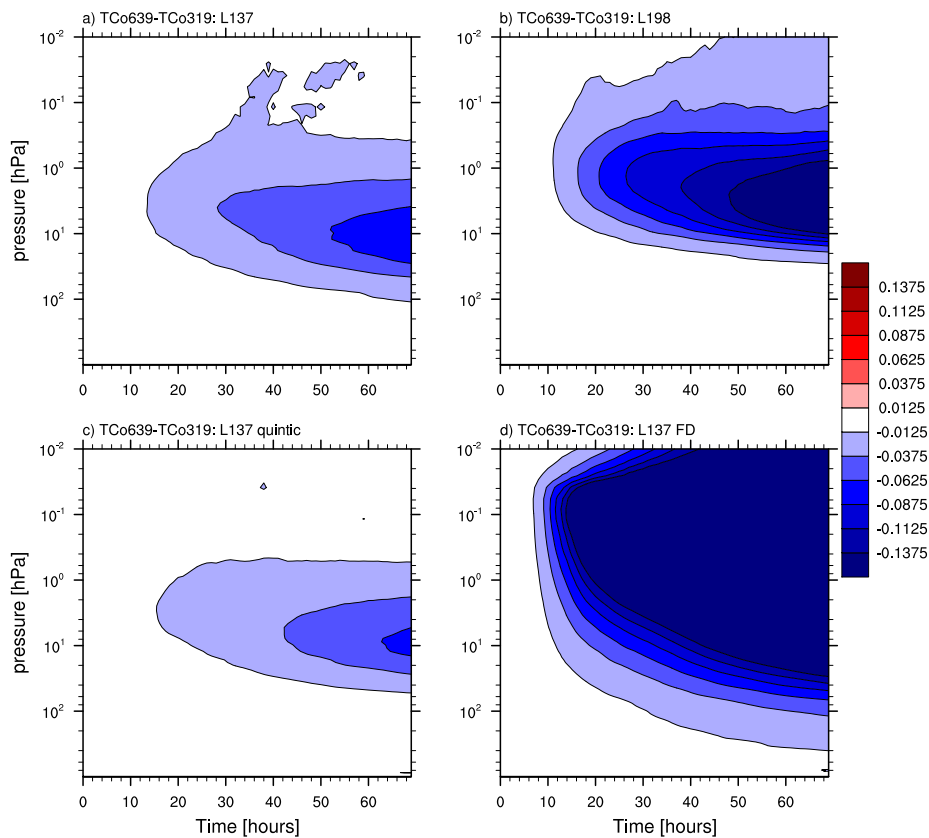


Figure 25: (a) Difference in global-mean temperature between *TCo639L137* and *TCo319L137* for Gaussian mountain test case simulations, as a function of pressure and lead time [in hours]. The high resolution simulation clearly loses more global-mean temperature. (b) Same as (a), but at *L198* vertical resolution. (c) Same as (a), but with quintic vertical interpolation on temperature. (d) Same as (a), but with finite difference instead of finite element vertical discretization.

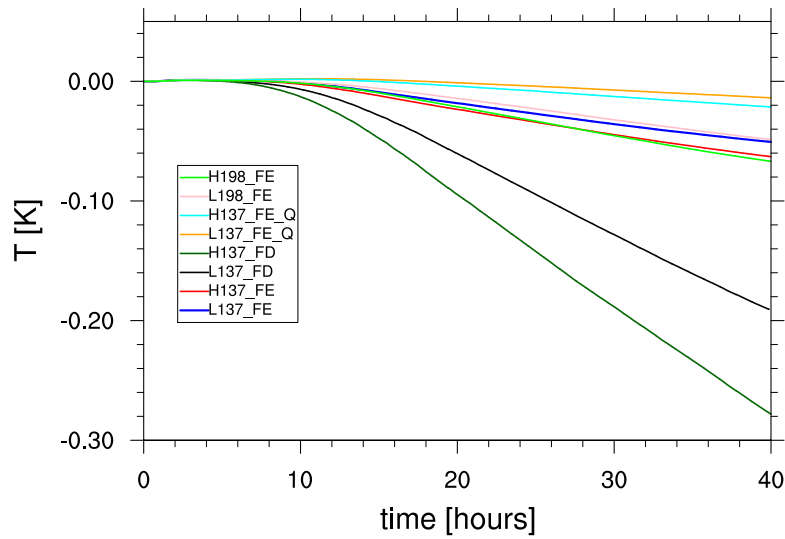


Figure 26: Departure of the global temperature-norm (norm over the whole domain, vertical and horizontal) from its initial value at  $t = 0$  Gaussian mountain test case, for different model settings. Finite element: TCo319L137 (blue), TCo639L137 (red), TCo319L198 (pink), and TCo639L198 (green). Finite difference; TCo319L137 (dark green) and TCo639L137 (black). Finite element with quintic vertical interpolation; TCo319L137 (orange) and TCo639L137 (cyan). ‘H’ refers to high, and, ‘L’ to low horizontal resolution.